

Published in final edited form as:

Nat Rev Neurosci. ; 13(1): 7–21. doi:10.1038/nrn3125.

Nanodomain coupling between Ca²⁺ channels and sensors of exocytosis at fast mammalian synapses

Emmanuel Eggermann, Iancu Bucurenciu, Sarit Pati Goswami, and Peter Jonas

IST Austria (Institute of Science and Technology Austria), Am Campus 1, A-3400 Klosterneuburg, Austria

Abstract

The physical distance between presynaptic Ca²⁺ channels and the Ca²⁺ sensors that trigger exocytosis of neurotransmitter-containing vesicles is a key determinant of the signalling properties of synapses in the nervous system. Recent functional analysis indicates that in some fast central synapses, transmitter release is triggered by a small number of Ca²⁺ channels that are coupled to Ca²⁺ sensors at the nanometre scale. Molecular analysis suggests that this tight coupling is generated by protein–protein interactions involving Ca²⁺ channels, Ca²⁺ sensors and various other synaptic proteins. Nanodomain coupling has several functional advantages, as it increases the efficacy, speed and energy efficiency of synaptic transmission.

Synaptic transmission involves a highly complex series of events. When an action potential invades a presynaptic terminal, Ca²⁺ inflow through voltage-gated Ca²⁺ channels leads to a rise in intracellular Ca²⁺ concentration. Next, Ca²⁺ binds to a presynaptic Ca²⁺ sensor, which subsequently triggers exocytosis of neurotransmitter-containing synaptic vesicles. Finally, the released transmitter diffuses across the synaptic cleft and binds to postsynaptic receptors. Thus, a voltage change in the presynaptic neuron (the action potential) is converted into two chemical signals (Ca²⁺ and transmitter) and then converted into an electrical response in the postsynaptic cell. Remarkably, what sounds like a lengthy sequence of slow biophysical and biochemical events takes place in less than a millisecond^{1–5}.

How such a short synaptic delay can be achieved is not completely understood. According to the laws of physics, diffusion time is proportional to the square of distance⁶. Thus, the high speed of synaptic transmission requires tight packing of the relevant molecules. The hypothesis that there is tight coupling between Ca²⁺ channels and Ca²⁺ sensors of exocytosis received initial support from experiments on two ‘classical’ synapses in the peripheral nervous system: the frog neuromuscular junction⁷ (FIG. 1a) and the squid giant synapse⁸ (FIG. 1b). At the frog neuromuscular junction, high-resolution electron microscopy tomography revealed that the distance between putative Ca²⁺ channels and synaptic vesicles was only ~20 nm (REF. 9) and modelling combined with cooperativity measurements suggested that vesicle fusion results from the Ca²⁺ inflow through only one or two Ca²⁺ channels¹⁰. Similarly, at the squid giant synapse, functional analysis indicated that the Ca²⁺ source and Ca²⁺ sensor are tightly coupled at nanometre distance¹¹ and only a few Ca²⁺

© 2012 Macmillan Publishers Limited. All rights reserved

Correspondence to P.J., peter.jonas@ist.ac.at.

Competing interests statement: The authors declare no competing financial interests.

FURTHER INFORMATION: Peter Jonas’s homepage : <http://www.ist.ac.at>

SUPPLEMENTARY INFORMATION: See online article: S1 (box)

channels are required for release^{12,13}. Evidence for both tight coupling and the involvement of a small number of channels has also been presented for the ciliary ganglion calyx synapses of the chick^{14,15}. In this uniquely accessible synaptic preparation, simultaneous electrophysiological recording from the transmitter release face of the calyx terminal and biochemical detection of transmitter release demonstrated that the opening of a single presynaptic Ca²⁺ channel can trigger exocytosis¹⁴.

Notably, all of these synapses have highly specialized properties and belong to peripheral nervous systems of invertebrates or lower vertebrates. Does nanodomain coupling also occur at synapses in the mammalian CNS? This is an important question for several reasons. First, detailed knowledge about coupling is essential to understand the biophysical factors shaping the efficacy and speed of synaptic transmission. Second, knowledge about coupling is necessary to correctly interpret the mechanisms of presynaptic forms of plasticity¹⁶ and the action of Ca²⁺ buffers¹⁷. Finally, obtaining an answer is important for understanding the mechanisms underlying information processing and coding in the brain. A definitive answer has been obtained only recently, after a range of central synapses were made accessible to quantitative biophysical analysis. These include the young and mature calyx of Held (a glutamatergic synapse in the auditory system^{18,19} (FIG. 1c)) and GABAergic synapses in the hippocampus and the cerebellum^{20,21} (FIG. 1d,e) that mediate fast feedforward and feedback inhibition in neuronal microcircuits.

In this Review, we summarize recent evidence for tight coupling between Ca²⁺ channels and Ca²⁺ sensors of exocytosis at central synapses, address the molecular mechanisms involved and discuss the functional implications of this coupling configuration.

Tight coupling at fast central synapses

The coupling distance between Ca²⁺ channels and Ca²⁺ sensors can be probed using the intracellular application of two exogenous Ca²⁺ chelators that have different binding rates (k_{on}), but comparable affinities (K_D) (TABLE 1). The basic principle is simple¹¹ (BOX 1). If the distance between Ca²⁺ channels and Ca²⁺ sensors of exocytosis is short (smaller than 100 nm), only the fast Ca²⁺ chelator BAPTA, but not the slow Ca²⁺ chelator EGTA, will have enough time to capture the Ca²⁺ on its way from the Ca²⁺ channels to the Ca²⁺ sensors and impair transmission in millimolar concentrations. By contrast, if the coupling distance is longer, both the fast and the slow Ca²⁺ chelator will be effective.

This approach has been applied to several synapses in the mammalian CNS, leading to surprising results. In the young calyx of Held (~8–10 days after birth) and in neocortical glutamatergic synapses (~14–16 days after birth), evoked transmitter release is suppressed by ~1 mM intracellular BAPTA, but also by ~10 mM EGTA^{3,22–25} (TABLE 2; FIG. 2a–c). This implies that the distance between Ca²⁺ channels and Ca²⁺ sensors must be long. At the young calyx of Held, quantitative modelling suggests that the average coupling distance is ~100 nm (range from 30 to 300 nm)²². Thus, evoked transmitter release at these synapses is triggered by so-called ‘Ca²⁺ microdomains’.

By contrast, at the output synapses of fast-spiking, parvalbumin-expressing GABAergic interneurons (basket cells) in the hippocampus (typically recorded ~18–21 days after birth), evoked transmitter release is inhibited by millimolar concentrations of BAPTA, but is largely unaffected by 30 mM EGTA²⁶ (TABLE 2; FIG. 2a–c). Furthermore, at the output synapses of inhibitory cells in the cerebellum, intracellular application of 1 mM EGTA has no effect on the proportion of synaptic failures²¹. Likewise, at cerebellar basket cell synapses, bath application of 20 μM of membrane-permeable EGTA acetoxymethyl ester (EGTA-AM) has only minimal effects on evoked transmitter release following a single presynaptic action potential²⁷. Although in the case of bath application of EGTA-AM the

concentration of intracellular EGTA is only roughly known²⁸, these results may suggest tight coupling between Ca^{2+} source and Ca^{2+} sensor. At the hippocampal basket cell-granule cell synapse, quantitative modelling reveals a uniform coupling distance in the range of 10–20 nm (REF. 26) (FIG. 2c). Thus, evoked transmitter release at fast hippocampal and cerebellar GABAergic synapses is triggered by ‘ Ca^{2+} nanodomains’.

Although the terms nanodomain and microdomain are widely used, their definitions are not very precise and have undergone historic shifts. Originally, the term microdomain was used to describe the high concentration of Ca^{2+} found near an open Ca^{2+} channel^{29–32}. Despite the name, these microdomains actually have spatial dimensions in the nanometre range (‘micro’ in ‘microdomain’ means ‘small’ in Greek). More recently, the terms nanodomain and microdomain have been widely applied to distinguish tight and loose coupling regimes. This definition is also confusing, as a limit of 50–150 nm is often used to separate between the two domains. Throughout this Review, we pragmatically refer to nanodomain coupling if the mean coupling distance is <100 nm, and to microdomain coupling if the distance is larger (BOX 1).

The Ca^{2+} chelator experiments not only suggest differences in the mean coupling distance but also in the uniformity of source–sensor coupling between synapses. In the young calyx of Held, 1 mM and 10 mM EGTA are almost equally effective^{3,22}. Accordingly, there is no single distance value that describes the concentration dependence of the chelator’s effects at this synapse³³. This suggests substantial non-uniformity in the coupling distance^{3,22}. This hypothesis is corroborated by uncaging experiments, which indicate that a subpopulation of vesicles in the calyx is reluctantly released following Ca^{2+} channel opening, but rapidly released by Ca^{2+} uncaging^{34,35}. By contrast, in the output synapses of hippocampal basket cells, a single coupling distance can adequately describe the effects of BAPTA and EGTA over a wide concentration range²⁶ (FIG. 2c). This suggests that the coupling is substantially more uniform²⁶. Consistent with this idea, the estimates of releasable pool sizes, as determined by action potential trains and sucrose application, differ at excitatory synapses but are comparable in inhibitory synapses³⁶. Thus, the tightness and uniformity of coupling at different synapses seem to be related.

The finding that the calyx of Held uses microdomain signalling for transmitter release^{3,22} was puzzling for several reasons. First, it was difficult to accept that two synapses with calyx morphology (the calyx of Held and the ciliary ganglion calyx) would differ fundamentally in the coupling configuration. Second, if tight coupling served the purpose of improving the speed and precision of transmitter release, it may be surprising that it is not utilized in the auditory system, where the timing of signalling is critically important. Indeed, analysis of coupling at the auditory hair cell ribbon synapse (the first station in the auditory pathway) revealed that transmitter release was blocked by intracellular BAPTA, but not EGTA, suggesting nanodomain coupling³⁷. Similar results were obtained at ribbon synapses in the visual system^{38,39}. A resolution of this apparent paradox was provided when coupling at the calyx of Held was examined at different developmental stages^{40,41}. In the mature calyx of Held (~16–18 days after birth), release is suppressed by millimolar concentrations of intracellular BAPTA, but is unaffected by 10 mM intracellular EGTA^{23,41} (TABLE 2). Modelling indicated that the coupling distance decreased to ~20 nm during development⁴², which is a similar distance to that at the hippocampal basket cell synapses. Thus, transmitter release at fast synapses in the mature auditory pathway is also triggered by Ca^{2+} nanodomains. Developmental processes may also regulate the tightness of coupling at glutamatergic^{24,25} and GABAergic synapses^{26,43} in the cortex. A systematic analysis of different synapses at different developmental stages is required to address this issue.

Specification and regulation of coupling

The results described above suggest that certain synapses in neuronal microcircuits (such as fast GABAergic output synapses of hippocampal or cerebellar basket cells) use nanodomain coupling, whereas others (such as glutamatergic synapses between layer 5 pyramidal neurons²⁴) involve microdomain coupling. These results raise two important questions. What are the rules that lead to the use of nanodomain signalling in one case and microdomain signalling in the other case, and is the coupling distance regulated dynamically?

Several lines of evidence suggest that synapses formed by different presynaptic neurons on the same target cell can use different coupling configurations. One example is provided by the opposite properties of synapses of parvalbumin- and cholecystokinin (CCK)-expressing interneurons onto hippocampal granule cells and pyramidal cells⁴³⁻⁴⁵. The fast-spiking, parvalbumin-expressing interneurons exhibit tight coupling, as confirmed by the lack of effect of external EGTA-AM, whereas the CCK-expressing interneurons show loose coupling, as demonstrated by the large effect of EGTA-AM on evoked release under identical experimental conditions^{26,43} (TABLE 2).

Furthermore, synapses formed by the same presynaptic neuron on different postsynaptic target cells can differ in their coupling configuration. The diverging output from layer 2/3 pyramidal neurons in the neocortex onto two types of interneurons provides a clear example²⁵. Layer 2/3 pyramidal neuron synapses on multipolar (presumably parvalbumin-expressing) interneurons are less sensitive to EGTA than synapses on bipolar (presumably somatostatin-expressing) interneurons (TABLE 2). These results may imply that a retrograde signalling mechanism regulates the tightness of the coupling in the presynaptic terminals.

Finally, the available results suggest that the use of nanodomain versus microdomain coupling may in some cases be pathway-specific. For example, both the input and the output synapses of parvalbumin-expressing interneurons use relatively tight coupling to trigger transmitter release^{25,26} (FIG. 2b,c,e). Likewise, both hair cells and mature calyces in the auditory system rely on nanodomain coupling^{23,46}. Thus, the tightness of coupling appears to be regulated in a pathway-specific manner. This regulation may be activity-dependent⁴⁷, but a more systematic analysis of different synapses, microcircuits and conditions will be needed to test this hypothesis.

An intriguing possibility is that the coupling between Ca²⁺ channels and Ca²⁺ sensors of exocytosis is not static, but is regulated dynamically. Recent results suggest that the induction of presynaptic long-term potentiation at distal perforant path synapses on CA1 pyramidal neurons is associated with an alteration in the dependence of transmitter release on P/Q- or N-type Ca²⁺ channels — resulting in an increased contribution of N-type Ca²⁺ channels after potentiation⁴⁸ (FIG. 2f). It is possible that these changes are connected to changes in channel–sensor coupling. Thus, dynamic regulation of the coupling distance may contribute to presynaptic forms of plasticity at central synapses⁴⁸.

In conclusion, the available evidence indicates that nanodomain coupling is regulated by both pre- and postsynaptic neurons, probably in a pathway-specific manner. Furthermore, recent results suggest that the coupling configuration is not static, but is regulated dynamically during presynaptic forms of synaptic plasticity. Further experiments will be needed to directly examine the dynamics of the coupling during presynaptic forms of plasticity.

How many Ca²⁺ channels for release?

Nanodomain coupling between Ca²⁺ channels and Ca²⁺ sensors places structural and functional constraints on the number of Ca²⁺ channels that can be involved in transmitter release. As voltage-gated Ca²⁺ channel proteins have a diameter of ~10 nm (REF. 49), the highest channel density that is physically possible is ~10,000 μm⁻². Accordingly, the number of Ca²⁺ channels involved in transmitter release in nanodomain coupling regimes must be small. For example, only ~12 channels can be placed on a planar presynaptic membrane within 20 nm from a synaptic vesicle. Furthermore, if coupling is tight, only a small number of Ca²⁺ channels may be needed to reach effective Ca²⁺ concentrations at the sensor.

How can one experimentally determine the number of open Ca²⁺ channels necessary for transmitter release? A classical approach is based on an analysis of the relationship between presynaptic Ca²⁺ inflow and transmitter release during an experimental reduction in the number of active Ca²⁺ channels. Such a reduction of Ca²⁺ channel number can be achieved either by application of slow Ca²⁺ channel blockers, such as peptide toxins⁵⁰, or by modifying the presynaptic voltage waveform that triggers exocytosis. The basic idea is relatively simple (BOX 2). If several open Ca²⁺ channels jointly trigger the release of a synaptic vesicle, the progressive reduction of Ca²⁺ inflow will lead to a supralinear reduction in transmitter release. This results from the so-called ‘intrinsic’ or ‘biochemical’ cooperativity⁵¹ of the Ca²⁺ sensor synaptotagmin, which has five binding sites for Ca²⁺ (REFS 52,53) and is expressed in multiple copies on each synaptic vesicle⁵⁴. By contrast, in the extreme case when only a single open Ca²⁺ channel triggers release of a synaptic vesicle, the slow blocker will reduce Ca²⁺ inflow and release proportionally.

This approach has recently been applied to various central synapses. At the young calyx of Held, the relationship between evoked transmitter release and presynaptic Ca²⁺ currents during slow Ca²⁺ channel block is highly supralinear, with a power coefficient (m) greater than 3, suggesting the involvement of a large number of open Ca²⁺ channels^{23,41,55}. By contrast, at the output synapses of hippocampal basket cells, the relationship is only slightly supralinear, with a power coefficient of 1.6 (REF. 56) (FIG. 2h,i). Modelling of experimental data with a binomial model of Ca²⁺ channel block suggested that two or three open Ca²⁺ channels trigger transmitter release at this synapse. Furthermore, in the mouse calyx of Held, the power coefficient is markedly reduced during development²³. Likewise, in the rat calyx, the power coefficient is slightly reduced during development and the relationship between transmitter release and Ca²⁺ charge is shifted to the left⁵⁷. Collectively, these results suggest that during development the number of open channels required for transmitter release is reduced, while the tightness of the coupling of these channels to their Ca²⁺ sensors is increased. Modelling also suggested the involvement of a small number of open Ca²⁺ channels in the mature calyx⁴². Finally, in both auditory hair cell ribbon synapses and retinal ribbon synapses, the relationship between evoked transmitter release and presynaptic Ca²⁺ during slow Ca²⁺ channel block shows a power coefficient of 1.1–1.4, also suggesting the involvement of a small number of open Ca²⁺ channels^{39,46,58}.

The involvement of a small number of open Ca²⁺ channels may be explained by two different configurations. In the first scenario, only a small number of Ca²⁺ channels are present at each active zone, but these channels are activated effectively by presynaptic action potentials. In the second scenario, the total Ca²⁺ channel number is large, but the efficacy of activation is low. In fast CNS synapses, the high efficacy of activation of P/Q- and N-type Ca²⁺ channels by action potentials (relative open probability 0.35–0.88 in different mammalian presynaptic terminals, including the calyx of Held)^{59–62} argues in

favour of the first scenario. By contrast, in the auditory hair cell synapses, the lower efficacy of activation of L-type Ca^{2+} channels would be more consistent with the second scenario⁴⁶.

These results converge towards a quantitative picture of signalling at fast central synapses. If an action potential invades a presynaptic structure, two or three Ca^{2+} channels near any given vesicle will open, generating a Ca^{2+} nanodomain. The Ca^{2+} concentration is high in the centre of the nanodomain, but steeply declines as a function of distance according to the laws of diffusion (Supplementary information S1 (box)). Thus, the Ca^{2+} sensor on the vesicle membrane would 'see' a Ca^{2+} transient with a high peak concentration and a fast time course, leading to vesicle fusion with high probability, short delay and high temporal precision. In this scenario, a 'release site'⁶³ would correspond to a channel-vesicle nanocomplex.

Ca^{2+} chelator experiments and cooperativity measurements provide additional constraints for the topographical arrangement of Ca^{2+} channels and vesicles in presynaptic terminals. First, they indicate that these nanocomplexes are sufficiently separated from their nearest neighbours so that their Ca^{2+} nanodomains do not overlap^{23,26,46,56}. Second, they suggest that nanocomplexes must be sufficiently far away from isolated Ca^{2+} channels that are not coupled to any synaptic vesicles. Finally, they imply that nanocomplexes are distant from isolated fusion competent vesicles that are not coupled to any Ca^{2+} channels³⁴. How could this segregation of Ca^{2+} channel-vesicle nanocomplexes be achieved? In basket cell synapses, which have small boutons with often a single active zone²⁶, nanocomplexes could be allocated to different boutons. At mature calyx synapses, which have ~600 active zones^{40,64}, or in auditory hair cells, which have ~15 active zones^{46,65}, nanocomplexes could be placed into different active zones of the same presynaptic terminal. However, sufficient separation may also be possible if nanocomplexes are located in different subregions of the same active zone. Active zones have a mean area of $\sim 0.1 \mu\text{m}^2$ ($0.094 \pm 0.01 \mu\text{m}^2$ in hippocampal basket cell synapses (A. Kulik, personal communication, and see REF. 26), $0.0996 \mu\text{m}^2$ in the young calyx⁶⁴, $0.0548 \mu\text{m}^2$ in the mature calyx⁴⁰ and $0.06 \mu\text{m}^2$ in auditory hair cells⁶⁵), which corresponds to the area of a circle with ~ 150 nm radius. If channel-vesicle nanocomplexes were preferentially placed in the periphery (for example, via protein-protein interactions) several of these complexes could be accommodated in a single active zone.

Nanodomains and endogenous Ca^{2+} buffers

The defining feature of nanodomain coupling is that the fast exogenous buffer BAPTA interferes with release at millimolar concentrations, whereas the slow exogenous buffer EGTA is ineffective¹⁷. This raises the question of how endogenous buffers act in nanodomain coupling regimes. A large number of Ca^{2+} buffers are present in presynaptic terminals of fast signalling synapses. These include parvalbumin in GABAergic synapses in the hippocampus, the cerebellum and the calyx of Held⁶⁶⁻⁶⁹, calretinin in the mature calyx of Held and auditory or vestibular hair cells^{70,71}, and calbindin in auditory hair cells^{66,72}. In addition, several proteins in the active zone have binding sites for Ca^{2+} . These include MUNC13 proteins, RAB3-interacting molecules (RIMs)¹⁰⁵ and the Ca^{2+} sensor synaptotagmin^{52,53}. Furthermore, several proteins enriched in the active zone contain binding sites for ubiquitously expressed Ca^{2+} -binding proteins. For example, P/Q-type Ca^{2+} channels have binding sites for calmodulin^{73,74}. Collectively, all of these proteins may contribute to the high endogenous buffer capacity of fast signalling neurons^{68,75}.

Can these endogenous Ca^{2+} -binding proteins affect nanodomain coupling? To address this question, information about concentration and Ca^{2+} -binding rate is required¹⁷. Recent evidence suggests that endogenous Ca^{2+} buffers can reach high (millimolar) concentrations.

Calibrated immunohistochemistry revealed that cerebellar basket cells express parvalbumin at a concentration of ~0.6 mM (REF. 76). Furthermore, single-cell protein content analysis demonstrated that vestibular hair cells contain calretinin at a concentration of ~1.2 mM (REF. 71). Finally, experiments with recombinant Ca²⁺ channels and tethered calmodulin mutants suggested a local calmodulin concentration as high as 2.5 mM (REF. 74). These Ca²⁺-binding proteins have 2–4 EF hand Ca²⁺ binding sites per molecule, resulting in high millimolar buffer concentrations in nanodomains. Recent results further suggest that the Ca²⁺-binding rate (k_{on}) of endogenous buffers may be faster than previously thought. For several Ca²⁺-binding proteins, the k_{on} values have now been quantified in Ca²⁺ uncaging experiments⁷⁷⁻⁷⁹. For both calretinin (relaxed form) and calbindin, k_{on} values are comparable to those of BAPTA⁷⁷⁻⁷⁹ (TABLE 1). For the calmodulin C-lobe (relaxed form), k_{on} is intermediate between BAPTA and EGTA, whereas for the calmodulin N-lobe, k_{on} is 100-fold higher than that of BAPTA⁷⁹ (TABLE 1). Finally, Ca²⁺ uncaging experiments suggest that k_{on} of the Ca²⁺ sensor synaptotagmin is comparable to that of BAPTA⁸⁰⁻⁸².

Taken together, these results indicate that many endogenous buffers are present at millimolar concentrations and have BAPTA-like binding properties, suggesting that they may interfere with nanodomain signalling. Several functional consequences are conceivable. First, fast endogenous buffers may reduce the amplitude of the Ca²⁺ transient, offering a mechanism to control the efficacy of synaptic transmission via regulation of buffer expression levels. Second, fast endogenous buffers will shorten the length constant of the buffer system, focusing the nanodomain in space. This effect may be particularly pronounced for fixed buffers (for example, calmodulin attached to presynaptic proteins), which will be saturated in the nanodomain, but unsaturated in the surround. This gradient of free buffer concentration may sharply focus the nanodomain in space⁸³. Finally, buffers may contribute to the use-dependency of presynaptic Ca²⁺ signalling^{25,83-87}. If presynaptic Ca²⁺ inflow during a first action potential saturates the buffer, the peak amplitude of a subsequent second Ca²⁺ transient will be facilitated relative to that of the first. Although facilitation of the Ca²⁺ transient is generally small, it will be amplified into a much larger facilitation of transmitter release because of intrinsic or biochemical cooperativity^{23,55,56,88}. For example, with a power coefficient of 3.3 (REF. 56), a 1.1-fold (10%) increase would result in a $(1.1)^{3.3} = 1.37$ -fold (37%) facilitation of release. Hence, endogenous Ca²⁺ buffers may regulate the amplitude, spatial extent and dynamics of Ca²⁺ nanodomains.

Among all Ca²⁺-binding proteins, parvalbumin appears to be a special case because its EF hand sites bind both Ca²⁺ and Mg²⁺ (REFS 89-91). Ca²⁺ binding exhibits fast on rate and high affinity, whereas Mg²⁺ binding is characterized by slower on rate and lower affinity. As the physiological cytoplasmic concentration of Mg²⁺ is high, Mg²⁺ has to unbind before Ca²⁺ can bind. Thus, parvalbumin may act as a slow buffer, in a similar way to the exogenous Ca²⁺ chelator EGTA^{90,91}. Furthermore, parvalbumin exhibits a higher mobility than other Ca²⁺-binding proteins^{92,93}. With all of these properties in mind, the tight correlation of parvalbumin expression with nanodomain signalling⁶⁷⁻⁷⁰ is highly perplexing. In some rapidly signalling synapses, the high total concentration of parvalbumin may provide a resolution to this apparent paradox. Although the fraction of free parvalbumin (the non-Mg²⁺-bound, non-Ca²⁺-bound state) under physiological conditions is <10%, the absolute concentration of the free buffer will be substantial under these conditions. This may have two consequences. First, parvalbumin may not exclusively act as a slow buffer (like EGTA)⁹⁰; it may also act like a fast buffer (like BAPTA) under physiological conditions⁷⁶. This explains how parvalbumin can affect synaptic transmission in tight coupling regimes^{21,68,76}. Second, the Mg²⁺-bound parvalbumin fraction will not primarily slow the effective Ca²⁺-binding rate, but rather contribute to the regeneration of free buffer. Therefore, Mg²⁺ binding/unbinding may establish a ‘metabuffering’ (that is, buffering of buffering) mechanism, thus maintaining the concentration of free parvalbumin during

repetitive activity in fast-spiking neurons. In parallel, the high mobility of parvalbumin will contribute to buffer regeneration in the nanodomain by rapid diffusion of free buffer from the periphery to the centre^{92,93}.

From nanodomains to protein complexes

A distance between Ca²⁺ channels and sensors of exocytosis of ~20 nm (REFS 26,42) is consistent with the idea that tight coupling is achieved by protein-protein interactions. Active zones are comprised of several evolutionarily conserved proteins, including members of the SNARE, RIM, ELKS and septin families⁹⁴. Recent results show that several of these proteins have a role in nanodomain coupling (FIG. 3).

The first presynaptic proteins shown to be involved in protein-protein interactions with presynaptic Ca²⁺ channels were the t-SNARE proteins, syntaxin and SNAP25. Both biochemical experiments (yeast two-hybrid experiments, co-immunoprecipitation and proteomic screens) and functional co-expression studies indicated that syntaxin and SNAP25 directly interact with voltage-gated Ca²⁺ channels at the intracellular loop between domains II and III of the channel protein, the so called 'synprint' site⁹⁵⁻⁹⁹. Synaptotagmin, the Ca²⁺ sensor that triggers exocytosis, also interacts with the synprint site in a Ca²⁺-dependent manner⁹⁵⁻⁹⁸. Intriguingly, the interactions between Ca²⁺ channels and SNARE proteins also affect Ca²⁺ channel function. Co-expression of syntaxin and SNAP25 with Ca²⁺ channels reduces the channel open probability, whereas additional co-expression of synaptotagmin reverses this effect⁹⁸. These results suggest a dual function for protein-protein interactions between Ca²⁺ channels and SNAREs in nanodomain coupling. First, they link the individual molecular elements within the nanodomain. Second, they establish a regulatory switch by which presynaptic Ca²⁺ channels bound to Ca²⁺ sensors are functionally selected, whereas Ca²⁺ channels decoupled from Ca²⁺ sensors are disabled.

Another protein that is relevant for the Ca²⁺ channel-sensor coupling is the *Drosophila melanogaster* protein Bruchpilot. Bruchpilot is a ~200 kDa active zone protein containing several coiled-coil domains¹⁰⁰. In the neuromuscular junctions of Bruchpilot knockout flies, synaptic efficacy is reduced and sensitivity to EGTA-AM is increased, suggesting a conversion from nanodomain to microdomain coupling¹⁰⁰. In mammalian synapses, two proteins homologous to Bruchpilot, ELKS/RAB6-interacting/CAST family member 1 (ERC1) and ERC2 are expressed. However, genetic elimination of ERC1 and ERC2 in mice has only moderate effects on synaptic function^{101,102}. Further studies will be required to clarify the exact role of ELKS proteins in the regulation of coupling at mammalian synapses.

α -neurexins also appear to be involved in the regulation of coupling between Ca²⁺ channels and Ca²⁺ sensors of exocytosis¹⁰³. Neurexins are 200 kDa polymorphic cell surface proteins with several epidermal growth factor (EGF) and laminin-neurexin-sex hormone binding globulin domains. They are encoded by three genes and expressed in ~1,000 isoforms. α -neurexins interact with neuroligins on the postsynaptic membrane and with both ELKS and synaptotagmin within the presynaptic terminal^{103,104}. Deletion of all three neurexin genes reduces evoked transmitter release and the contribution of N-type Ca²⁺ channels to release at synapses in brainstem and cortex¹⁰³, consistent with a role for α -neurexins in the regulation of Ca²⁺ channel-sensor coupling. Neurexin-neuroligin interactions may potentially explain the target cell specificity of coupling²⁵. Ca²⁺ chelator experiments in neurexin knockout synapses will be needed to test this idea.

Recent results suggest that RIMs have a central organizing role in regulating the coupling between Ca²⁺ channels and Ca²⁺ sensors of exocytosis^{105,106} (FIG. 3b-d). RIMs are multidomain proteins that contain a PDZ domain that selectively interacts with the C terminus of P/Q- and N-type channels. RIMs also contain a binding site for the RIM-binding

proteins (RIM-BPs), which in turn binds to several Ca^{2+} channel subtypes¹⁰⁷. Thus, RIMs establish two links to voltage-gated Ca^{2+} channels: a direct and specific link, and an indirect and unselective link via RIM-BP. In inhibitory hippocampal synapses in culture, genetic elimination of RIM1 and RIM2 reduces the amplitude of evoked inhibitory postsynaptic currents, desynchronizes release, accelerates the onset of the blocking effects of EGTA-AM and shifts the dependence of release on extracellular Ca^{2+} concentration to higher values¹⁰⁵ (FIG. 3c,d). Taken together, these results suggest that the coupling between Ca^{2+} channels and Ca^{2+} sensors of exocytosis is disrupted in RIM1 and RIM2 double knockout synapses. Similarly, in the calyx of Held, genetic elimination of RIM1 and RIM2 reduces both the presynaptic Ca^{2+} channel density and the amplitude of the Ca^{2+} transient at the Ca^{2+} sensor¹⁰⁶. Additionally, RIM1 and RIM2 knockout may also affect the number of docked and primed vesicles^{105,106}. Thus, at both inhibitory hippocampal synapses and the calyx of Held, RIMs seem to be crucially involved in the regulation of the coupling between Ca^{2+} channels and Ca^{2+} sensors of exocytosis.

Finally, the presynaptic GTP/GDP- and syntaxin-binding protein septin regulates the coupling between Ca^{2+} channels and Ca^{2+} sensors^{108,109}. Septins are ~35 kDa proteins that form oligomers and higher order structures, such as filaments, rings and gauzes. Septins may form filaments between synaptic vesicles and active zones¹¹⁰. In the young calyx of Held, genetic elimination of septin 5 reduces the sensitivity to EGTA, suggesting a conversion from microdomain to nanodomain coupling¹⁰⁹. Two aspects of the function of septin 5 are remarkable. First, unlike other presynaptic proteins, septin 5 increases the coupling distance, suggesting antagonistic control of coupling by presynaptic proteins. Second, the expression of septin 5 is downregulated during development, suggesting an involvement in the developmental switch from microdomain to nanodomain coupling at the calyx¹⁰⁹.

Intriguingly, the tightness of the coupling not only depends on various release machinery proteins but also on the Ca^{2+} channel subtype. In basket cell output synapses of the hippocampus and cerebellum, as well as in the mature calyx of Held, tight coupling goes hand-in-hand with the nearly exclusive use of P/Q-type Ca^{2+} channels for transmitter release^{43,56,111-113}. By contrast, loose coupling is often correlated with the involvement of N- or R-type Ca^{2+} channels^{43,55}. Additionally, there is evidence that P/Q- and N-type Ca^{2+} channels populate partially non-overlapping 'slots' within the active zone of glutamatergic synapses¹¹⁴. Finally, L-type Ca^{2+} channels (rather than P/Q-, N- or R-type Ca^{2+} channels) are tightly coupled to their Ca^{2+} sensors in auditory hair cells^{37,46}. Clearly, this coupling specificity cannot be mediated by the synprint site, which follows an efficacy sequence of $\text{N} > \text{P/Q} > \text{L}$ ^{115,116}. Thus, the molecular mechanisms underlying this specificity remain unclear.

Nanodomain: advantage, bug or feature?

What are the functional consequences of nanodomain coupling? This question can be systematically addressed by modelling, combining simulation of buffered diffusion (Supplementary information S1 (box)) with previously established models of Ca^{2+} channel gating^{59,60} and Ca^{2+} sensor kinetics^{80-82,117,118} (Supplementary information S1 (box)).

Modelling revealed that nanodomain coupling offers several functional advantages, but may also have disadvantages. The long list of obvious advantages includes increased efficacy and speed of synaptic transmission (FIG. 4a–c). First, tight coupling reduces the synaptic delay^{22,26}. Although the reduction in delay is small for a monosynaptic connection (~100 μs), cumulative effects are expected in polysynaptic chains. Second, tight coupling reduces the duration of the release period, as the time course of the Ca^{2+} transient 'seen' by the Ca^{2+} sensor is faster in nanodomain than in microdomain coupling regimes. Third, tight coupling

increases the ratio of peak Ca^{2+} to residual Ca^{2+} and hence the ratio of synchronous to asynchronous release^{26,43,119}. Therefore, in relative terms, tight coupling reduces asynchronous release. This effect may be particularly important in small boutons, in which residual Ca^{2+} concentration after an action potential is higher than in large presynaptic terminals. Finally, another advantage of nanodomain coupling is that release outside the active zone ('ectopic release') is minimized^{120,121}.

As tight coupling of a small number of channels to the Ca^{2+} sensors reduces the total Ca^{2+} inflow into presynaptic terminals, this configuration is also favourable for the energetics of synaptic transmission (FIG. 4d). Ca^{2+} extrusion from the presynaptic terminal involves either $\text{Na}^+/\text{Ca}^{2+}$ exchangers or Ca^{2+} -ATPases¹²². In both cases, the extrusion of one Ca^{2+} ion requires the hydrolysis of ~1 ATP molecule. A coupling configuration in which a small number of Ca^{2+} channels are tightly coupled to presynaptic Ca^{2+} sensors therefore reduces the metabolic cost of synaptic transmission. Such an energy-saving mechanism may be important at GABAergic synapses in the cortex and at glutamatergic synapses in the auditory pathway, which are active at high frequencies under physiological conditions *in vivo*.

A potential disadvantage of nanodomain coupling with a small number of Ca^{2+} channels could be an additional 'jitter' of evoked transmitter release caused by the stochastic opening of presynaptic Ca^{2+} channels^{15,22} (FIG. 4e). However, whereas the opening and closing of Ca^{2+} channels is stochastic, the rising phase of the corresponding Ca^{2+} transient evoked by an overshooting action potential is largely deterministic, governed by the increase in driving force during the repolarization phase^{56,123} (FIG. 4e). Thus, transmitter release remains tightly synchronized, even if evoked release is triggered by only a small number of Ca^{2+} channels.

Another potential disadvantage of nanodomain coupling is that stochastic openings of Ca^{2+} channels at rest might trigger spontaneous transmitter release¹⁵ (FIG. 4f). However, recent results in dentate gyrus granule cells suggest that blocking P/Q-type Ca^{2+} channels with ω -agatoxin IVa has no effect on miniature inhibitory postsynaptic current (IPSC) frequency, although evoked release at basket cell–granule cell synapses exclusively relies on P/Q-type Ca^{2+} channels¹²⁴. Furthermore, BAPTA-AM and EGTA-AM reduce miniature IPSC frequency to the same extent, suggesting that microdomains rather than nanodomains trigger spontaneous release¹²⁴. Thus, the high activation threshold and steep voltage dependence of P/Q-type Ca^{2+} channels, and the use of two or three open Ca^{2+} channels rather than a single channel, may protect the synapse from excessive spontaneous release generated by stochastic Ca^{2+} channel opening^{56,60}.

Nanodomain coupling also has substantial implications for synaptic dynamics, promoting synaptic depression over synaptic facilitation for two reasons. First, for any given number of channels, it increases release probability and thus enhances depression owing to depletion of the releasable pool of synaptic vesicles. Second, it reduces facilitation by decreasing the relative weight of residual Ca^{2+} (REF. 125). Consistent with these effects, the fast signalling synapses that rely on nanodomain coupling often show depression during high-frequency stimulus trains, albeit to a different extent¹⁹⁻²¹.

Finally, nanodomain coupling will have implications for how neuromodulators affect the release of neurotransmitters and how they interact with synaptic dynamics. Previous studies suggested that presynaptic G-protein-coupled receptors (such as presynaptic GABA_B receptors) reduce the activity of P/Q- and N-type Ca^{2+} channels via binding of G-protein β - and γ -subunits to Ca^{2+} channels¹²⁶. In nanodomain coupling regimes, this will have two consequences. First, the reduction in transmitter release will be largely proportional to the

degree of presynaptic receptor activation. This may allow a more precise regulation of synaptic efficacy than a highly supralinear relationship. Second, as presynaptic receptor activation will reduce the number of Ca^{2+} channel-vesicle nanocomplexes but will not affect release probability, the neuromodulators will not affect short-term dynamics, resulting in scaling of synaptic responses during repetitive stimulation, as observed in the hippocampus¹²⁷ (but see REF. 142 for observations in the neocortex).

Conclusions

Twenty years after the original finding of nanodomain coupling at the squid giant synapse¹¹, and after a subsequent decade of accumulating evidence for microdomain coupling at central synapses¹²⁸, it has become clear that synapses in the mammalian CNS also make extensive use of nanodomain coupling for fast transmitter release. In particular, GABAergic interneuron output synapses and glutamatergic synapses in the auditory pathway rely on nanodomain coupling. Nanodomain coupling provides several functional advantages, including efficacy, speed and energy efficiency of synaptic transmission. How abundantly nanodomain coupling is used by different synapses in the mammalian CNS remains to be addressed. Furthermore, the rules of synapse specificity of nanodomain coupling remain to be determined. Finally, it will be interesting to see whether nanodomain coupling between Ca^{2+} channels and Ca^{2+} sensors of exocytosis is disrupted in neurological or psychiatric diseases¹²⁹.

Supplementary Material

Refer to Web version on PubMed Central for supplementary material.

Acknowledgments

We thank D. Tsien and E. Neher for their comments on this Review, J. Guzmán and A. Pernía-Andrade for reading earlier versions and E. Kramberger for perfect editorial support. Work of the authors was funded by grants of the Deutsche Forschungsgemeinschaft to P.J. (grants SFB 780/A5, TR 3/B10 and the Leibniz programme), a European Research Council Advanced grant to P.J. and a Swiss National Foundation fellowship to E.E. We apologize that owing to space constraints, not all relevant papers could be cited.

Glossary

Synaptic delay	The time interval between the presynaptic action potential and the postsynaptic response. A synaptic delay is comprised of several components: opening of presynaptic Ca^{2+} channels, diffusion of Ca^{2+} from the channels to the Ca^{2+} sensors, activation of Ca^{2+} sensors, exocytosis, diffusion of transmitter across the synaptic cleft and activation of postsynaptic receptors.
Ca^{2+} chelators	Chemical substances that bind Ca^{2+} . In synaptic physiology, BAPTA and EGTA are widely used Ca^{2+} chelators. Both chelators are also available in membrane-permeable acetoxymethyl ester (AM) forms.
BAPTA	1,2-bis(2-aminophenoxy) ethane-N,N,N',N'-tetraacetic acid
EGTA	ethylene glycol-bis(2-aminoethylether)-N,N,N',N'-tetraacetic acid

Ca²⁺ microdomains	Domains of elevated Ca ²⁺ concentration that extend over more than 100 nanometres. Note that this definition does not imply that the size of the domain is in the micrometre range (1 μm = 10 ⁻⁶ m).
Basket cells	Types of perisomatic inhibitory GABAergic interneurons in the hippocampus and cerebellum. The name was given as the axon forms ‘baskets’ around somata of postsynaptic target cells.
Ca²⁺ nanodomains	Domains of elevated Ca ²⁺ concentration that extend over less than 100 nanometres (1 nm = 10 ⁻⁹ m).
Intrinsic or biochemical cooperativity	Nonlinear dependence of transmitter release on the intracellular Ca ²⁺ concentration, presumably owing to multiple Ca ²⁺ -binding sites on the Ca ²⁺ sensor synaptotagmin and multiple copies of synaptotagmin on individual synaptic vesicles.
Rab3-interacting molecules (RIMs)	Active zone proteins that serve as central organizers, tethering presynaptic Ca ²⁺ channels and Ca ²⁺ sensors of exocytosis. RIMs are encoded by four genes, which drive the expression of seven known isoforms. For synaptic transmission, only the long RIM versions are relevant.
Length constant	The distance in which a quantity declines to the fraction 1/e. In the case of buffered diffusion of Ca ²⁺ , the length constant represents the mean distance Ca ²⁺ diffuses before it is captured by the buffer.
Fixed buffers	Fixed buffers always remain at the same location. In contrast to mobile buffers, fixed buffers can only be regenerated by Ca ²⁺ unbinding, not by diffusion.
SNARE	Soluble <i>N</i> -ethylmaleimide-sensitive-factor attachment protein (SNAP) receptor.
ELKS	Glutamic acid, leucine, lysine and serine-rich protein (also known as cytomatrix of the active zone-associated structural protein (CAST)).
Synaptic depression	Decrease in efficacy of synaptic transmission during and after stimulation of the presynaptic neuron. Synaptic depression is often interpreted as a depletion of the releasable pool of synaptic vesicles, although other mechanisms such as changes in presynaptic action potential shape and inactivation of presynaptic Ca ²⁺ channels may also contribute.
Synaptic facilitation	Short-lasting increase in efficacy of synaptic transmission during and after repetitive stimulation. Synaptic facilitation is often attributed to residual Ca ²⁺ following the action potential, although other mechanisms such as saturation of endogenous buffers may also contribute.

References

1. Katz B, Miledi R. The measurement of synaptic delay, and the time course of acetylcholine release at the neuromuscular junction. *Proc. R. Soc. Lond. B.* 1965; 161:483–495. [PubMed: 14278409]

2. Llinás R, Sugimori M, Simon SM. Transmission by presynaptic spike-like depolarization in the squid giant synapse. *Proc. Natl Acad. Sci. USA.* 1982; 79:2415–2419. [PubMed: 6954549]
3. Borst JGG, Sakmann B. Calcium influx and transmitter release in a fast CNS synapse. *Nature.* 1996; 383:431–434. [PubMed: 8837774]
4. Sabatini BL, Regehr WG. Timing of neurotransmission at fast synapses in the mammalian brain. *Nature.* 1996; 384:170–172. [PubMed: 8906792]
5. Geiger JRP, Jonas P. Dynamic control of presynaptic Ca^{2+} inflow by fast-inactivating K^+ channels in hippocampal mossy fiber boutons. *Neuron.* 2000; 28:927–939. [PubMed: 11163277]
6. Einstein A. Über die von der molekularkinetischen Theorie der Wärme geforderte Bewegung von in ruhenden Flüssigkeiten suspendierten Teilchen. *Annalen der Physik.* 1905; 17:549–560.
7. Katz, B. *The Release of Neural Transmitter Substances.* Liverpool Univ. Press; Liverpool: 1969.
8. Llinás, RR. *The Squid Giant Synapse.* Oxford Univ. Press; New York: 1999.
9. Harlow ML, Ress D, Stoschek A, Marshall RM, McMahan UJ. The architecture of active zone material at the frog's neuromuscular junction. *Nature.* 2001; 409:479–484. [PubMed: 11206537] [A classical electron microscopy tomography study of the active zone at the frog neuromuscular junction. Four rows of presynaptic Ca^{2+} channels are opposed to two rows of synaptic vesicles, with ~20 nm between the individual elements.]
10. Shahrezaei V, Cao A, Delaney KR. Ca^{2+} from one or two channels controls fusion of a single vesicle at the frog neuromuscular junction. *J. Neurosci.* 2006; 26:13240–13249. [PubMed: 17182774] [The authors cleverly exploit the advantage of the Monte-Carlo simulation to monitor individual Ca^{2+} ions. By backtracing the Ca^{2+} from the vesicle to the Ca^{2+} channels through which they entered, the authors conclude that only one or two open Ca^{2+} channels contribute to transmitter release at the frog neuromuscular junction.]
11. Adler EM, Augustine GJ, Duffy SN, Charlton MP. Alien intracellular calcium chelators attenuate neurotransmitter release at the squid giant synapse. *J. Neurosci.* 1991; 11:1496–1507. [PubMed: 1675264] [A classical paper that uses exogenous Ca^{2+} chelators with different binding rates to probe the distance between Ca^{2+} source and Ca^{2+} sensor at the squid giant synapse. Based on the lack of effects of the slow Ca^{2+} chelator EGTA, the authors suggest that nanodomain coupling exists between Ca^{2+} channels and Ca^{2+} sensors at this invertebrate synapse.]
12. Augustine GJ. Regulation of transmitter release at the squid giant synapse by presynaptic delayed rectifier potassium current. *J. Physiol.* 1990; 431:343–364. [PubMed: 1983120]
13. Augustine GJ, Adler EM, Charlton MP. The calcium signal for transmitter secretion from presynaptic nerve terminals. *Ann. NY Acad. Sci.* 1991; 635:365–381. [PubMed: 1683754]
14. Stanley EF. Single calcium channels and acetylcholine release at a presynaptic nerve terminal. *Neuron.* 1993; 11:1007–1011. [PubMed: 8274272] [The first direct evidence that a single Ca^{2+} channel triggers exocytosis at a chick calyx synapse. In enzymatically treated preparations, the release face of the calyx (that is, the side that is normally attached to the postsynaptic ciliary neuron) is sometimes partially separated from the postsynaptic cell, allowing simultaneous electrophysiological recording of presynaptic Ca^{2+} channel activity and chemoluminescent detection of acetylcholine release.]
15. Stanley EF. The calcium channel and the organization of the presynaptic transmitter release face. *Trends Neurosci.* 1997; 20:404–409. [PubMed: 9292969]
16. Nicoll RA, Schmitz D. Synaptic plasticity at hippocampal mossy fibre synapses. *Nature Rev. Neurosci.* 2005; 6:863–876. [PubMed: 16261180]
17. Neher E. Usefulness and limitations of linear approximations to the understanding of Ca^{++} signals. *Cell Calcium.* 1998; 24:345–357. [PubMed: 10091004]
18. Forsythe ID. Direct patch recording from identified presynaptic terminals mediating glutamatergic EPSCs in the rat CNS, *in vitro*. *J. Physiol.* 1994; 479:381–387. [PubMed: 7837096]
19. von Gersdorff H, Borst JGG. Short-term plasticity at the calyx of Held. *Nature Rev. Neurosci.* 2002; 3:53–64. [PubMed: 11823805]
20. Kraushaar U, Jonas P. Efficacy and stability of quantal GABA release at a hippocampal interneuron-principal neuron synapse. *J. Neurosci.* 2000; 20:5594–5607. [PubMed: 10908596]
21. Caillard O, et al. Role of the calcium-binding protein parvalbumin in short-term synaptic plasticity. *Proc. Natl Acad. Sci. USA.* 2000; 97:13372–13377. [PubMed: 11069288]

22. Meinrenken CJ, Borst JGG, Sakmann B. Calcium secretion coupling at calyx of Held governed by nonuniform channel-vesicle topography. *J. Neurosci.* 2002; 22:1648–1667. [PubMed: 11880495]
23. Fedchyshyn MJ, Wang LY. Developmental transformation of the release modality at the calyx of Held synapse. *J. Neurosci.* 2005; 25:4131–4140. [PubMed: 15843616] [This paper demonstrates a developmental decrease of sensitivity of evoked transmitter release to EGTA at the calyx of Held, indicating a tightening of Ca^{2+} channel–sensor coupling. Furthermore, it shows a reduction in Ca^{2+} current cooperativity during development. Although the power coefficients in this study cannot be correlated to the number of open channels required for release (they exceed the upper bound of biochemical cooperativity), the results may indicate a reduction of this number during development.]
24. Ohana O, Sakmann B. Transmitter release modulation in nerve terminals of rat neocortical pyramidal cells by intracellular calcium buffers. *J. Physiol.* 1998; 513:135–148. [PubMed: 9782165]
25. Rozov A, Burnashev N, Sakmann B, Neher E. Transmitter release modulation by intracellular Ca^{2+} buffers in facilitating and depressing nerve terminals of pyramidal cells in layer 2/3 of the rat neocortex indicates a target cell-specific difference in presynaptic calcium dynamics. *J. Physiol.* 2001; 531:807–826. [PubMed: 11251060] [This paper reports that the Ca^{2+} chelator BAPTA induces pseudofacilitation. Careful quantitative analysis reveals buffer saturation as the underlying mechanism.]
26. Bucurenciu I, Kulik A, Schwaller B, Frotscher M, Jonas P. Nanodomain coupling between Ca^{2+} channels and Ca^{2+} sensors promotes fast and efficient transmitter release at a cortical GABAergic synapse. *Neuron.* 2008; 57:536–545. [PubMed: 18304483]
27. Christie JM, Chiu DN, Jahr CE. Ca^{2+} -dependent enhancement of release by subthreshold somatic depolarization. *Nature Neurosci.* 2011; 14:62–68. [PubMed: 21170054]
28. Atluri PP, Regehr WG. Determinants of the time course of facilitation at the granule cell to Purkinje cell synapse. *J. Neurosci.* 1996; 16:5661–5671. [PubMed: 8795622]
29. Chad JE, Eckert R. Calcium domains associated with individual channels can account for anomalous voltage relations of Ca-dependent responses. *Biophys. J.* 1984; 45:993–999. [PubMed: 6329349]
30. Llinás R, Sugimori M, Silver RB. Microdomains of high calcium concentration in a presynaptic terminal. *Science.* 1992; 256:677–679. [PubMed: 1350109]
31. Fogelson AL, Zucker RS. Presynaptic calcium diffusion from various arrays of single channels. Implications for transmitter release and synaptic facilitation. *Biophys. J.* 1985; 48:1003–1017. [PubMed: 2418887]
32. Roberts WM. Localization of calcium signals by a mobile calcium buffer in frog saccular hair cells. *J. Neurosci.* 1994; 14:3246–3262. [PubMed: 8182469]
33. Naraghi M, Neher E. Linearized buffered Ca^{2+} diffusion in microdomains and its implications for calculation of $[\text{Ca}^{2+}]$ at the mouth of a calcium channel. *J. Neurosci.* 1997; 17:6961–6973. [PubMed: 9278532]
34. Wadel K, Neher E, Sakaba T. The coupling between synaptic vesicles and Ca^{2+} channels determines fast neurotransmitter release. *Neuron.* 2007; 53:563–575. [PubMed: 17296557]
35. Neher E, Sakaba T. Multiple roles of calcium ions in the regulation of neurotransmitter release. *Neuron.* 2008; 59:861–872. [PubMed: 18817727]
36. Moulder KL, Mennerick S. Reluctant vesicles contribute to the total readily releasable pool in glutamatergic hippocampal neurons. *J. Neurosci.* 2005; 25:3842–3850. [PubMed: 15829636]
37. Moser T, Beutner D. Kinetics of exocytosis and endocytosis at the cochlear inner hair cell afferent synapse of the mouse. *Proc. Natl Acad. Sci. USA.* 2000; 97:883–888. [PubMed: 10639174]
38. Mennerick S, Matthews G. Ultrafast exocytosis elicited by calcium current in synaptic terminals of retinal bipolar neurons. *Neuron.* 1996; 17:1241–1249. [PubMed: 8982170]
39. Jarsky T, Tian M, Singer JH. Nanodomain control of exocytosis is responsible for the signaling capability of a retinal ribbon synapse. *J. Neurosci.* 2010; 30:11885–11895. [PubMed: 20826653]
40. Taschenberger H, Leão RM, Rowland KC, Spiro GA, von Gersdorff H. Optimizing synaptic architecture and efficiency for high-frequency transmission. *Neuron.* 2002; 36:1127–1143. [PubMed: 12495627]

41. Wang LY, Neher E, Taschenberger H. Synaptic vesicles in mature calyx of Held synapses sense higher nanodomain calcium concentrations during action potential-evoked glutamate release. *J. Neurosci.* 2008; 28:14450–14458. [PubMed: 19118179]
42. Wang LY, Fedchyshyn MJ, Yang YM. Action potential evoked transmitter release in central synapses: insights from the developing calyx of Held. *Mol. Brain.* 2009; 2:36. [PubMed: 19939269]
43. Hefft S, Jonas P. Asynchronous GABA release generates long-lasting inhibition at a hippocampal interneuron-principal neuron synapse. *Nature Neurosci.* 2005; 8:1319–1328. [PubMed: 16158066]
44. Glickfeld LL, Scanziani M. Distinct timing in the activity of cannabinoid-sensitive and cannabinoid-insensitive basket cells. *Nature Neurosci.* 2006; 9:807–815. [PubMed: 16648849]
45. Daw MI, Tricoire L, Erdelyi F, Szabo G, McBain CJ. Asynchronous transmitter release from cholecystokinin-containing inhibitory interneurons is widespread and target-cell independent. *J. Neurosci.* 2009; 29:11112–11122. [PubMed: 19741117]
46. Brandt A, Khimich D, Moser T. Few $\text{Ca}_v1.3$ channels regulate the exocytosis of a synaptic vesicle at the hair cell ribbon synapse. *J. Neurosci.* 2005; 25:11577–11585. [PubMed: 16354915] [Evidence that a few Ca^{2+} channels trigger exocytosis at auditory hair cell ribbon synapses.]
47. Erazo-Fischer E, Striessnig J, Taschenberger H. The role of physiological afferent nerve activity during *in vivo* maturation of the calyx of Held synapse. *J. Neurosci.* 2007; 27:1725–1737. [PubMed: 17301180]
48. Ahmed MS, Siegelbaum SA. Recruitment of N-type Ca^{2+} channels during LTP enhances low release efficacy of hippocampal CA1 perforant path synapses. *Neuron.* 2009; 63:372–385. [PubMed: 19679076] [This paper shows that distal perforant path synapses on CA1 pyramidal neurons exhibit a presynaptic form of long-term potentiation dependent on Ca^{2+} channel recruitment. This may suggest that the coupling between Ca^{2+} channels and transmitter release is altered during presynaptic forms of plasticity.]
49. Pumplin DW, Reese TS, Llinás R. Are the presynaptic membrane particles the calcium channels? *Proc. Natl Acad. Sci. USA.* 1981; 78:7210–7213. [PubMed: 6273920]
50. Yoshikami D, Bagabaldo Z, Olivera BM. The inhibitory effects of omega-conotoxins on Ca channels and synapses. *Ann. NY Acad. Sci.* 1989; 560:230–248. [PubMed: 2545135]
51. Matveev V, Bertram R, Sherman A. Ca^{2+} current versus Ca^{2+} channel cooperativity of exocytosis. *J. Neurosci.* 2009; 29:12196–12209. [PubMed: 19793978]
52. Chapman ER. How does synaptotagmin trigger neurotransmitter release? *Annu. Rev. Biochem.* 2008; 77:615–641. [PubMed: 18275379]
53. Pang ZP, Südhof TC. Cell biology of Ca^{2+} -triggered exocytosis. *Curr. Opin. Cell Biol.* 2010; 22:496–505. [PubMed: 20561775]
54. Takamori S, et al. Molecular anatomy of a trafficking organelle. *Cell.* 2006; 127:831–846. [PubMed: 17110340] [A classical paper that quantitatively determines the protein content of synaptic vesicles. Among other proteins, 15 synaptotagmin copies and ten RAB3A copies are present per vesicle.]
55. Wu LG, Westenbroek RE, Borst JGG, Catterall WA, Sakmann B. Calcium channel types with distinct presynaptic localization couple differentially to transmitter release in single calyx-type synapses. *J. Neurosci.* 1999; 19:726–736. [PubMed: 9880593]
56. Bucurenciu I, Bischofberger J, Jonas P. A small number of open Ca^{2+} channels trigger transmitter release at a central GABAergic synapse. *Nature Neurosci.* 2010; 13:19–21. [PubMed: 20010820]
57. Kochubey O, Han Y, Schneggenburger R. Developmental regulation of the intracellular Ca^{2+} sensitivity of vesicle fusion and Ca^{2+} -secretion coupling at the rat calyx of Held. *J. Physiol.* 2009; 587:3009–3023. [PubMed: 19403608]
58. von Gersdorff H, Sakaba T, Berglund K, Tachibana M. Submillisecond kinetics of glutamate release from a sensory synapse. *Neuron.* 1998; 21:1177–1188. [PubMed: 9856472]
59. Borst JGG, Sakmann B. Calcium current during a single action potential in a large presynaptic terminal of the rat brainstem. *J. Physiol.* 1998; 506:143–157. [PubMed: 9481678]
60. Li L, Bischofberger J, Jonas P. Differential gating and recruitment of P/Q-, N-, and R-type Ca^{2+} channels in hippocampal mossy fiber boutons. *J. Neurosci.* 2007; 27:13420–13429. [PubMed: 18057200]

61. Yang YM, Wang LY. Amplitude and kinetics of action potential-evoked Ca^{2+} current and its efficacy in triggering transmitter release at the developing calyx of Held synapse. *J. Neurosci.* 2006; 26:5698–5708. [PubMed: 16723526]
62. Lin KH, Oleskevich S, Taschenberger H. Presynaptic Ca^{2+} influx and vesicle exocytosis at the mouse endbulb of Held: a comparison of two auditory nerve terminals. *J. Physiol.* 2011; 589:4301–4320. [PubMed: 21746778]
63. Stevens CF. Neurotransmitter release at central synapses. *Neuron.* 2003; 40:381–388. [PubMed: 14556715]
64. Sätzler K, et al. Three-dimensional reconstruction of a calyx of Held and its postsynaptic principal neuron in the medial nucleus of the trapezoid body. *J. Neurosci.* 2002; 22:10567–10579. [PubMed: 12486149]
65. Roberts WM, Jacobs RA, Hudspeth AJ. Colocalization of ion channels involved in frequency selectivity and synaptic transmission at presynaptic active zones of hair cells. *J. Neurosci.* 1990; 10:3664–3684. [PubMed: 1700083]
66. Celio MR. Calbindin D-28k and parvalbumin in the rat nervous system. *Neuroscience.* 1990; 35:375–475. [PubMed: 2199841]
67. Freund TF, Buzsáki G. Interneurons of the hippocampus. *Hippocampus.* 1996; 6:347–470. [PubMed: 8915675]
68. Collin T, et al. Developmental changes in parvalbumin regulate presynaptic Ca^{2+} signaling. *J. Neurosci.* 2005; 25:96–107. [PubMed: 15634771]
69. Müller M, Felmy F, Schwaller B, Schneggenburger R. Parvalbumin is a mobile presynaptic Ca^{2+} buffer in the calyx of Held that accelerates the decay of Ca^{2+} and short-term facilitation. *J. Neurosci.* 2007; 27:2261–2271. [PubMed: 17329423]
70. Felmy F, Schneggenburger R. Developmental expression of the Ca^{2+} -binding proteins calretinin and parvalbumin at the calyx of Held of rats and mice. *Eur. J. Neurosci.* 2004; 20:1473–1482. [PubMed: 15355314]
71. Edmonds B, Reyes R, Schwaller B, Roberts WM. Calretinin modifies presynaptic calcium signaling in frog saccular hair cells. *Nature Neurosci.* 2000; 3:786–790. [PubMed: 10903571]
72. Hackney CM, Mahendrasingam S, Penn A, Fettiplace R. The concentrations of calcium buffering proteins in mammalian cochlear hair cells. *J. Neurosci.* 2005; 25:7867–7875. [PubMed: 16120789]
73. Lee A, Zhou H, Scheuer T, Catterall WA. Molecular determinants of Ca^{2+} /calmodulin-dependent regulation of $\text{Ca}_v2.1$ channels. *Proc. Natl Acad. Sci. USA.* 2003; 100:16059–16064. [PubMed: 14673106]
74. Mori MX, Erickson MG, Yue DT. Functional stoichiometry and local enrichment of calmodulin interacting with Ca^{2+} channels. *Science.* 2004; 304:432–435. [PubMed: 15087548]
75. Aponte Y, Bischofberger J, Jonas P. Efficient Ca^{2+} buffering in fast-spiking basket cells of rat hippocampus. *J. Physiol.* 2008; 586:2061–2075. [PubMed: 18276734]
76. Eggermann E, Jonas P. How the ‘slow’ Ca^{2+} buffer parvalbumin affects transmitter release in nanodomain-coupling regimes. *Nature Neurosci.* Dec 4.2011 doi:10.1038/nn.3002.
77. Nägerl UV, Novo D, Mody I, Vergara JL. Binding kinetics of calbindin-D_{28k} determined by flash photolysis of caged Ca^{2+} *Biophys. J.* 2000; 79:3009–3018. [PubMed: 11106608]
78. Faas GC, Schwaller B, Vergara JL, Mody I. Resolving the fast kinetics of cooperative binding: Ca^{2+} buffering by calretinin. *PLoS Biol.* 2007; 5:e311. [PubMed: 18044987]
79. Faas GC, Raghavachari S, Lisman JE, Mody I. Calmodulin as a direct detector of Ca^{2+} signals. *Nature Neurosci.* 2011; 14:301–304. [PubMed: 21258328] [This paper measures the Ca^{2+} -binding rates of different Ca^{2+} -binding proteins directly, using fast Ca^{2+} uncaging in a cuvette. Surprisingly, the binding rate for the N-lobe of calmodulin (relaxed form) is even faster than that of BAPTA.]
80. Schneggenburger R, Neher E. Intracellular calcium dependence of transmitter release rates at a fast central synapse. *Nature.* 2000; 406:889–893. [PubMed: 10972290]
81. Bollmann JH, Sakmann B, Borst JGG. Calcium sensitivity of glutamate release in a calyx-type terminal. *Science.* 2000; 289:953–957. [PubMed: 10937999]
82. Lou X, Scheuss V, Schneggenburger R. Allosteric modulation of the presynaptic Ca^{2+} sensor for vesicle fusion. *Nature.* 2005; 435:497–501. [PubMed: 15917809]

83. Nowycky MC, Pinter MJ. Time courses of calcium and calcium-bound buffers following calcium influx in a model cell. *Biophys. J.* 1993; 64:77–91. [PubMed: 8431551]
84. Matveev V, Zucker RS, Sherman A. Facilitation through buffer saturation: constraints on endogenous buffering properties. *Biophys. J.* 2004; 86:2691–2709. [PubMed: 15111389]
85. Jackson MB, Redman SJ. Calcium dynamics, buffering, and buffer saturation in the boutons of dentate granule-cell axons in the hilus. *J. Neurosci.* 2003; 23:1612–1621. [PubMed: 12629165]
86. Blatow M, Caputi A, Burnashev N, Monyer H, Rozov A. Ca^{2+} buffer saturation underlies paired pulse facilitation in calbindin-D28k-containing terminals. *Neuron.* 2003; 38:79–88. [PubMed: 12691666]
87. Felmy F, Neher E, Schneggenburger R. Probing the intracellular calcium sensitivity of transmitter release during synaptic facilitation. *Neuron.* 2003; 37:801–811. [PubMed: 12628170]
88. Dodge FA, Rahamimoff R. Co-operative action of calcium ions in transmitter release at the neuromuscular junction. *J. Physiol.* 1967; 193:419–432. [PubMed: 6065887]
89. Lee SH, Schwaller B, Neher E. Kinetics of Ca^{2+} binding to parvalbumin in bovine chromaffin cells: implications for $[\text{Ca}^{2+}]$ transients of neuronal dendrites. *J. Physiol.* 2000; 525:419–432. [PubMed: 10835044]
90. Schwaller B, Meyer M, Schiffmann S. 'New' functions for 'old' proteins: the role of the calcium-binding proteins calbindin D-28k, calretinin and parvalbumin, in cerebellar physiology. Studies with knockout mice. *Cerebellum.* 2002; 1:241–258. [PubMed: 12879963]
91. Schwaller B. Cytosolic Ca^{2+} buffers. *Cold Spring Harb. Perspect. Biol.* 2010; 2:a004051. [PubMed: 20943758]
92. Schmidt H, Brown EB, Schwaller B, Eilers J. Diffusional mobility of parvalbumin in spiny dendrites of cerebellar Purkinje neurons quantified by fluorescence recovery after photobleaching. *Biophys. J.* 2003; 84:2599–2608. [PubMed: 12668468] [This paper directly measures the diffusion coefficient of the Ca^{2+} -binding protein parvalbumin from the time course of recovery of fluorescence after photobleaching. Unlike many other Ca^{2+} -binding proteins, parvalbumin is highly mobile.]
93. Schmidt H, Schwaller B, Eilers J. Calbindin D28k targets myo-inositol monophosphatase in spines and dendrites of cerebellar Purkinje neurons. *Proc. Natl Acad. Sci. USA.* 2005; 102:5850–5855. [PubMed: 15809430]
94. Müller CS, et al. Quantitative proteomics of the Cav2 channel nano-environments in the mammalian brain. *Proc. Natl Acad. Sci. USA.* 2010; 107:14950–14957. [PubMed: 20668236]
95. Sheng ZH, Yokoyama CT, Catterall WA. Interaction of the synprint site of N-type Ca^{2+} channels with the C2B domain of synaptotagmin I. *Proc. Natl Acad. Sci. USA.* 1997; 94:5405–5410. [PubMed: 9144250]
96. Bezprozvanny I, Scheller RH, Tsien RW. Functional impact of syntaxin on gating of N-type and Q-type calcium channels. *Nature.* 1995; 378:623–626. [PubMed: 8524397]
97. Rettig J, et al. Isoform-specific interaction of the $\alpha 1A$ subunits of brain Ca^{2+} channels with the presynaptic proteins syntaxin and SNAP-25. *Proc. Natl Acad. Sci. USA.* 1996; 93:7363–7368. [PubMed: 8692999]
98. Zhong H, Yokoyama CT, Scheuer T, Catterall WA. Reciprocal regulation of P/Q-type Ca^{2+} channels by SNAP-25, syntaxin and synaptotagmin. *Nature Neurosci.* 1999; 2:939–941. [PubMed: 10526329]
99. Atlas D. Functional and physical coupling of voltage-sensitive calcium channels with exocytotic proteins: ramifications for the secretion mechanism. *J. Neurochem.* 2001; 77:972–985. [PubMed: 11359862]
100. Kittel RJ, et al. Bruchpilot promotes active zone assembly, Ca^{2+} channel clustering, and vesicle release. *Science.* 2006; 312:1051–1054. [PubMed: 16614170]
101. Wang Y, Liu X, Biederer T, Südhof TC. A family of RIM-binding proteins regulated by alternative splicing: implications for the genesis of synaptic active zones. *Proc. Natl. Acad. Sci. USA.* 2002; 99:14464–14469. [PubMed: 12391317]
102. Kaeser PS, et al. ELKS2 α /CAST deletion selectively increases neurotransmitter release at inhibitory synapses. *Neuron.* 2009; 64:227–239. [PubMed: 19874790]

103. Missler M, et al. α -neurexins couple Ca^{2+} channels to synaptic vesicle exocytosis. *Nature*. 2003; 423:939–948. [PubMed: 12827191]
104. Boucard AA, Chubykin AA, Comoletti D, Taylor P, Südhof TC. A splice code for trans-synaptic cell adhesion mediated by binding of neuroligin 1 to α - and β -neurexins. *Neuron*. 2005; 48:229–236. [PubMed: 16242404]
105. Kaeser PS, et al. RIM proteins tether Ca^{2+} channels to presynaptic active zones via a direct PDZ-domain interaction. *Cell*. 2011; 144:282–295. [PubMed: 21241895] [This paper shows that RIM acts as a tethering molecule linking presynaptic Ca^{2+} channels to the exocytosis machinery.]
106. Han Y, Kaeser PS, Südhof TC, Schneggenburger R. RIM determines Ca^{2+} channel density and vesicle docking at the presynaptic active zone. *Neuron*. 2011; 69:304–316. [PubMed: 21262468]
107. Hibino H, et al. RIM binding proteins (RBPs) couple Rab3-interacting molecules (RIMs) to voltage-gated Ca^{2+} channels. *Neuron*. 2002; 34:411–423. [PubMed: 11988172]
108. Beites CL, Xie H, Bowser R, Trimble WS. The septin CDCrel-1 binds syntaxin and inhibits exocytosis. *Nature Neurosci*. 1999; 2:434–439. [PubMed: 10321247]
109. Yang YM, et al. Septins regulate developmental switching from microdomain to nanodomain coupling of Ca^{2+} influx to neurotransmitter release at a central synapse. *Neuron*. 2010; 67:100–115. [PubMed: 20624595]
110. Siksou L, et al. Three-dimensional architecture of presynaptic terminal cytomatrix. *J. Neurosci*. 2007; 27:6868–6877. [PubMed: 17596435]
111. Iwasaki S, Takahashi T. Developmental changes in calcium channel types mediating synaptic transmission in rat auditory brainstem. *J. Physiol*. 1998; 509:419–423. [PubMed: 9575291]
112. Forti L, Pouzat C, Llano I. Action potential-evoked Ca^{2+} signals and calcium channels in axons of developing rat cerebellar interneurons. *J. Physiol*. 2000; 527:33–48. [PubMed: 10944168]
113. Stephens GJ, Morris NP, Fyffe REW, Robertson B. The Cav2.1/ α 1A (P/Q-type) voltage-dependent calcium channel mediates inhibitory neurotransmission onto mouse cerebellar Purkinje cells. *Eur. J. Neurosci*. 2001; 13:1902–1912. [PubMed: 11403683]
114. Cao YQ, Tsien RW. Different relationship of N- and P/Q-type Ca^{2+} channels to channel-interacting slots in controlling neurotransmission at cultured hippocampal synapses. *J. Neurosci*. 2010; 30:4536–4546. [PubMed: 20357104]
115. Mochida S, Westenbroek RE, Yokoyama CT, Itoh K, Catterall WA. Subtype-selective reconstitution of synaptic transmission in sympathetic ganglion neurons by expression of exogenous calcium channels. *Proc. Natl Acad. Sci. USA*. 2003; 100:2813–2818. [PubMed: 12601155]
116. Mochida S, et al. Requirement for the synaptic protein interaction site for reconstitution of synaptic transmission by P/Q-type calcium channels. *Proc. Natl Acad. Sci. USA*. 2003; 100:2819–2824. [PubMed: 12601156]
117. Sun J, et al. A dual- Ca^{2+} -sensor model for neurotransmitter release in a central synapse. *Nature*. 2007; 450:676–682. [PubMed: 18046404]
118. Sakaba T. Two Ca^{2+} -dependent steps controlling synaptic vesicle fusion and replenishment at the cerebellar basket cell terminal. *Neuron*. 2008; 57:406–419. [PubMed: 18255033]
119. Atluri PP, Regehr WG. Delayed release of neurotransmitter from cerebellar granule cells. *J. Neurosci*. 1998; 18:8214–8227. [PubMed: 9763467]
120. Matsui K, Jahr CE. Ectopic release of synaptic vesicles. *Neuron*. 2003; 40:1173–1183. [PubMed: 14687551] [This paper shows that EGTA-AM leaves synaptic release on Purkinje cells unaffected, but inhibits ectopic release on Bergmann glial cells. This suggests that synaptic release is triggered by Ca^{2+} nanodomains, whereas ectopic release is driven by Ca^{2+} microdomains.]
121. Matsui K, Jahr CE. Differential control of synaptic and ectopic vesicular release of glutamate. *J. Neurosci*. 2004; 24:8932–8939. [PubMed: 15483112]
122. Kim MH, Korogod N, Schneggenburger R, Ho WK, Lee SH. Interplay between $\text{Na}^+/\text{Ca}^{2+}$ exchangers and mitochondria in Ca^{2+} clearance at the calyx of Held. *J. Neurosci*. 2005; 25:6057–6065. [PubMed: 15987935]
123. Ribault C, Sekimoto K, Triller A. From the stochasticity of molecular processes to the variability of synaptic transmission. *Nature Rev. Neurosci*. 2011; 12:375–387. [PubMed: 21685931]

124. Goswami, SP.; Jonas, P.; Bucurenciu, I. Soc. Neurosci. Abstr. Washington DC: Nov 12-16. 2011 Differential dependence of miniature IPSC and EPSC frequency on presynaptic Ca^{2+} channels at hippocampal synapses; p. 446.07
125. Zucker RS, Regehr WG. Short-term synaptic plasticity. *Annu. Rev. Physiol.* 2002; 64:355–405. [PubMed: 11826273]
126. Bean BP. Neurotransmitter inhibition of neuronal calcium currents by changes in channel voltage dependence. *Nature.* 1989; 340:153–156. [PubMed: 2567963]
127. Hefft S, Kraushaar U, Geiger JRP, Jonas P. Presynaptic short-term depression is maintained during regulation of transmitter release at a GABAergic synapse in rat hippocampus. *J. Physiol.* 2002; 539:201–208. [PubMed: 11850513]
128. Meinrenken CJ, Borst JGG, Sakmann B. Local routes revisited: the space and time dependence of the Ca^{2+} signal for phasic transmitter release at the rat calyx of Held. *J. Physiol.* 2003; 547:665–689. [PubMed: 12562955]
129. Cao YQ, et al. Presynaptic Ca^{2+} channels compete for channel type-preferring slots in altered neurotransmission arising from Ca^{2+} channelopathy. *Neuron.* 2004; 43:387–400. [PubMed: 15294146]
130. Lansman JB, Hess P, Tsien RW. Blockade of current through single calcium channels by Cd^{2+} , Mg^{2+} , and Ca^{2+} . Voltage and concentration dependence of calcium entry into the pore. *J. Gen. Physiol.* 1986; 88:321–347. [PubMed: 2428920]
131. Wheeler DB, Randall A, Tsien RW. Roles of N-type and Q-type Ca^{2+} channels in supporting hippocampal synaptic transmission. *Science.* 1994; 264:107–111. [PubMed: 7832825]
132. Castillo PE, Weisskopf MG, Nicoll RA. The role of Ca^{2+} channels in hippocampal mossy fiber synaptic transmission and long-term potentiation. *Neuron.* 1994; 12:261–269. [PubMed: 8110457]
133. Mintz IM, Sabatini BL, Regehr WG. Calcium control of transmitter release at a cerebellar synapse. *Neuron.* 1995; 15:675–688. [PubMed: 7546746]
134. Bertram R, Smith GD, Sherman A. Modeling study of the effects of overlapping Ca^{2+} microdomains on neurotransmitter release. *Biophys. J.* 1999; 76:735–750. [PubMed: 9929478] [A detailed modelling paper that cleans up several misconceptions regarding the cooperativity of Ca^{2+} inflow and transmitter release.]
135. Wu LG, Saggau P. Pharmacological identification of two types of presynaptic voltage-dependent calcium channels at CA3-CA1 synapses of the hippocampus. *J. Neurosci.* 1994; 14:5613–5622. [PubMed: 8083757]
136. Bullock TH, Hagiwara S. Intracellular recording from the giant synapse of the squid. *J. Gen. Physiol.* 1957; 40:565–577. [PubMed: 13416531]
137. Nicholls, JG.; Martin, RA.; Wallace, B, G. From Neuron to Brain. Sinauer, Sunderland, Massachusetts, USA: 1992.
138. Pernía-Andrade A, Jonas P. The multiple faces of RIM. *Neuron.* 2011; 69:185–187. [PubMed: 21262457]
139. Naraghi M. T-jump study of calcium binding kinetics of calcium chelators. *Cell Calcium.* 1997; 22:255–268. [PubMed: 9481476]
140. Singer JH, Diamond JS. Sustained Ca^{2+} entry elicits transient postsynaptic currents at a retinal ribbon synapse. *J. Neurosci.* 2003; 23:10923–10933. [PubMed: 14645488]
141. Borst JGG, Helmchen F, Sakmann B. Pre- and postsynaptic whole-cell recordings in the medial nucleus of the trapezoid body of the rat. *J. Physiol.* 1995; 489:825–840. [PubMed: 8788946]
142. Kruglikov I, Rudy B. Perisomatic GABA release and thalamocortical integration onto neocortical excitatory cells are regulated by neuromodulators. *Neuron.* 2008; 58:911–924. [PubMed: 18579081]

Box 1**Probing nanodomains and microdomains with exogenous Ca²⁺ chelators**

The distance between Ca²⁺ source and Ca²⁺ sensor can be probed using Ca²⁺ chelators with different Ca²⁺-binding rates (k_{on}), but comparable affinities (K_D)¹¹. Ca²⁺ chelators suppress synaptic transmission by intercepting the Ca²⁺ on its way from the Ca²⁺ source to the Ca²⁺ sensor (FIG. 2a). The exact amount of block depends on source-sensor distance, binding rate and concentration of the chelator. If the coupling distance is short, only the fast Ca²⁺ chelator will have an effect at millimolar concentrations. If the coupling distance is long, both fast and slow Ca²⁺ chelators will be effective, according to their affinity at equilibrium. This approach was first applied to the squid giant synapse¹¹ using the fast chelator BAPTA and the slow chelator EGTA. BAPTA and EGTA are ideal experimental tools because they differ by a factor of ~40 in their on rates, but show comparable affinity values^{22,33,77,139} (TABLE 1).

The concentration dependence of the BAPTA and EGTA effects provides information about the average coupling distance between Ca²⁺ channels and Ca²⁺ sensors. Such data may be used to distinguish between nanodomain and microdomain coupling regimes. The concentration dependence of the chelator effects also provides information about the uniformity of the coupling distance. For example, at the young calyx of Held, the concentration dependence determined experimentally can only be described by theoretical models if significant non-uniformity in the coupling distance is assumed²².

Although the terms nanodomain and microdomain are widely used, they are not precisely defined. What is the distance limit between nanodomains and microdomains? One approach is to use the border between diffusion regimes and buffering regimes as a criterion (for example, by choosing a distance where buffering reduces the Ca²⁺ concentration to 50%). This can be roughly estimated from the length constant (λ) of endogenous buffers.

With $\lambda = \sqrt{D_{Ca} / (k_{on} [B])}$, where $D_{Ca} = 220 \mu\text{m}^2 \text{s}^{-1}$ (REF. 17), $k_{on} = 10^8 \text{M}^{-1} \text{s}^{-1}$ (an on rate representative of endogenous buffers (TABLE 1)) and $[B] = 100 \mu\text{M}$, $[\text{Ca}^{2+}]_{50\%}$ is reached at a distance of 100 nm. Alternatively, the limit may be set according to vesicle size and active zone size. As the radius of synaptic vesicles is ~20 nm (REF. 64) and the radius of active zones is typically ~150 nm (REFS 26,40,64,65), the limit should be set in between. Throughout this Review, we define the border between nanodomain and microdomain at a distance of 100 nm.

Box 2**Counting the number of release-relevant Ca²⁺ channels**

The number of open Ca²⁺ channels required for transmitter release can be determined from the shape of the relationship between release and presynaptic Ca²⁺ inflow^{12,13,56}. In synapses where presynaptic voltage clamp is possible, the number of open channels can be manipulated by varying the amplitude and duration of the depolarization²³. Under these conditions, the presynaptic Ca²⁺ current can be directly recorded. In other synapses where presynaptic voltage clamp is not possible, the number of Ca²⁺ channels can be changed by application of channel blockers^{50,56}. Under these conditions, presynaptic Ca²⁺ inflow is quantified by Ca²⁺ imaging. The results from these measurements then give the relationship between transmitter release and presynaptic Ca²⁺ inflow. If a large number of open Ca²⁺ channels are required for transmitter release, the relationship will be supralinear, approaching the biochemical cooperativity of the Ca²⁺ sensor (FIG. 2g). By contrast, if a single open Ca²⁺ channel is sufficient to trigger transmitter release, the relationship will be linear because the blocker will sequentially eliminate channel-vesicle nanocomplexes (FIG. 2g). If the number of channels is small, but >1, the shape of the relationship will be intermediate between these two extremes.

Evidently, the power coefficient of the release-Ca²⁺ inflow relationship is not identical to the number of open Ca²⁺ channels necessary for transmitter release. To quantitatively determine this number, modelling has to be performed⁵⁶. If blockers are used, a simple binomial model of Ca²⁺ channel block can be chosen. However, several factors must be considered. The properties of the blocker are crucial: the ideal blocker should have slow kinetics and block Ca²⁺ channels uniformly throughout the presynaptic terminal. Fast blockers that generate a flicker block¹³⁰ or blockers that reduce the single-channel conductance cannot be used. The techniques for measuring presynaptic Ca²⁺ inflow and transmitter release have to be quantitative and linear. The modelling is based on several assumptions, such as uniform coupling distance and independent block of channels, which may not be valid in all cases. It must also be kept in mind that the method measures the number of open channels, not the total number of Ca²⁺ channels present. These two numbers can substantially differ because the maximal open probability of Ca²⁺ channels during presynaptic action potentials is significantly smaller than one⁵⁹⁻⁶². This approach has been successfully applied to synapses where transmitter release exclusively relies on a single type of Ca²⁺ channel, such as the P/Q-type Ca²⁺ channel in GABAergic synapses^{43,56} or the L-type Ca²⁺ channel in auditory hair cell ribbon synapses⁴⁶. At synapses where transmitter release relies on the concerted action of P/Q-, N- and R-type channels^{55,131-133}, careful interpretation of the results is required. If release-[Ca²⁺] relationships are measured using subtype-specific blockers, the results will provide information about channel location rather than number. If channels are loosely coupled, they will contribute little to release (low power coefficient), whereas if they are tightly coupled, they will contribute more (high power coefficient)¹³⁴. Thus, the power coefficients, although informative, are entirely unrelated to channel numbers. By contrast, non-additive blocker effects may provide indirect information about channel number. Evidence for non-additive blocker effects was reported at the young calyx of Held⁵⁵, glutamatergic synapses in the hippocampus^{131,132,135} and glutamatergic parallel fibre synapses in the cerebellum¹³³. In these synapses, the sum of the effects of individual blockers on transmitter release is larger than 100%, suggesting the involvement of a large number of channels.

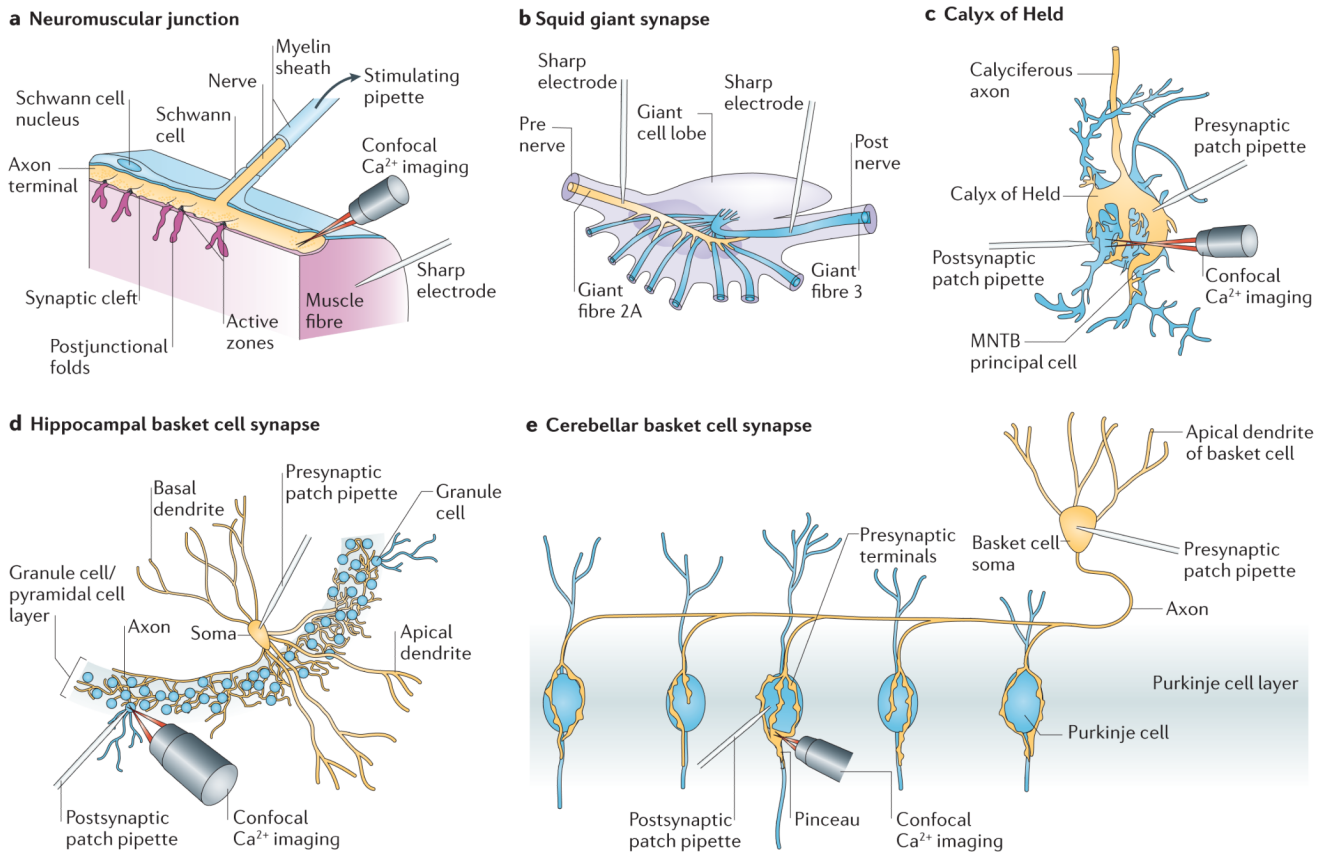


Figure 1. Model synapses used for the analysis of Ca²⁺ channel-sensor coupling

a | The frog neuromuscular junction, which is a classical preparation for the analysis of synaptic transmission⁷. This synapse is formed between motor axons (yellow) and skeletal muscle fibres (pink). A technical advantage is the 1:1 innervation (1 motor axon:1 muscle fibre). Furthermore, the structure of this synapse has been studied extensively⁹. Presynaptic access, however, is not possible. **b** | The squid giant synapse⁸. This synapse is established between second and third order giant nerve fibres in the stellate ganglion of the squid¹³⁶. A technical advantage is that presynaptic elements can be recorded directly with sharp microelectrodes. **c** | The calyx of Held in the auditory brainstem^{18,19}. This synapse is formed between the globular bushy cells in the cochlear nucleus and the neurons of the medial nucleus of the trapezoid body (MNTB)¹⁹. A technical advantage of this synapse is that presynaptic terminals can be recorded directly with patch-clamp techniques. However, a disadvantage is that recordings from older animals (>postnatal day 8–10) are difficult. **d** | The hippocampal dentate gyrus basket cell synapse²⁰. This synapse is established between fast-spiking, parvalbumin-expressing basket cells in the hippocampus (yellow) and postsynaptic target cells (in this case granule cells, blue). **e** | The cerebellar basket cell synapse²¹. This synapse is established between parvalbumin-expressing basket cells in the cerebellum (yellow) and postsynaptic target cells (in this case Purkinje cells, blue). In hippocampal and cerebellar basket cell synapses, paired recordings between presynaptic and postsynaptic neurons can be obtained with high success rates because of the relatively high connectivity. A disadvantage of these synapses is that presynaptic terminals cannot be routinely recorded. Part **a** is modified, with permission, from REF. 137 © (1992) Sinauer. Part **b** is modified, with permission, from REF. 136 © (1957) The Rockefeller University

Press. Part **e** is modified, with permission, from REF. 19 © (2002) Macmillan Publishers Ltd. All rights reserved.

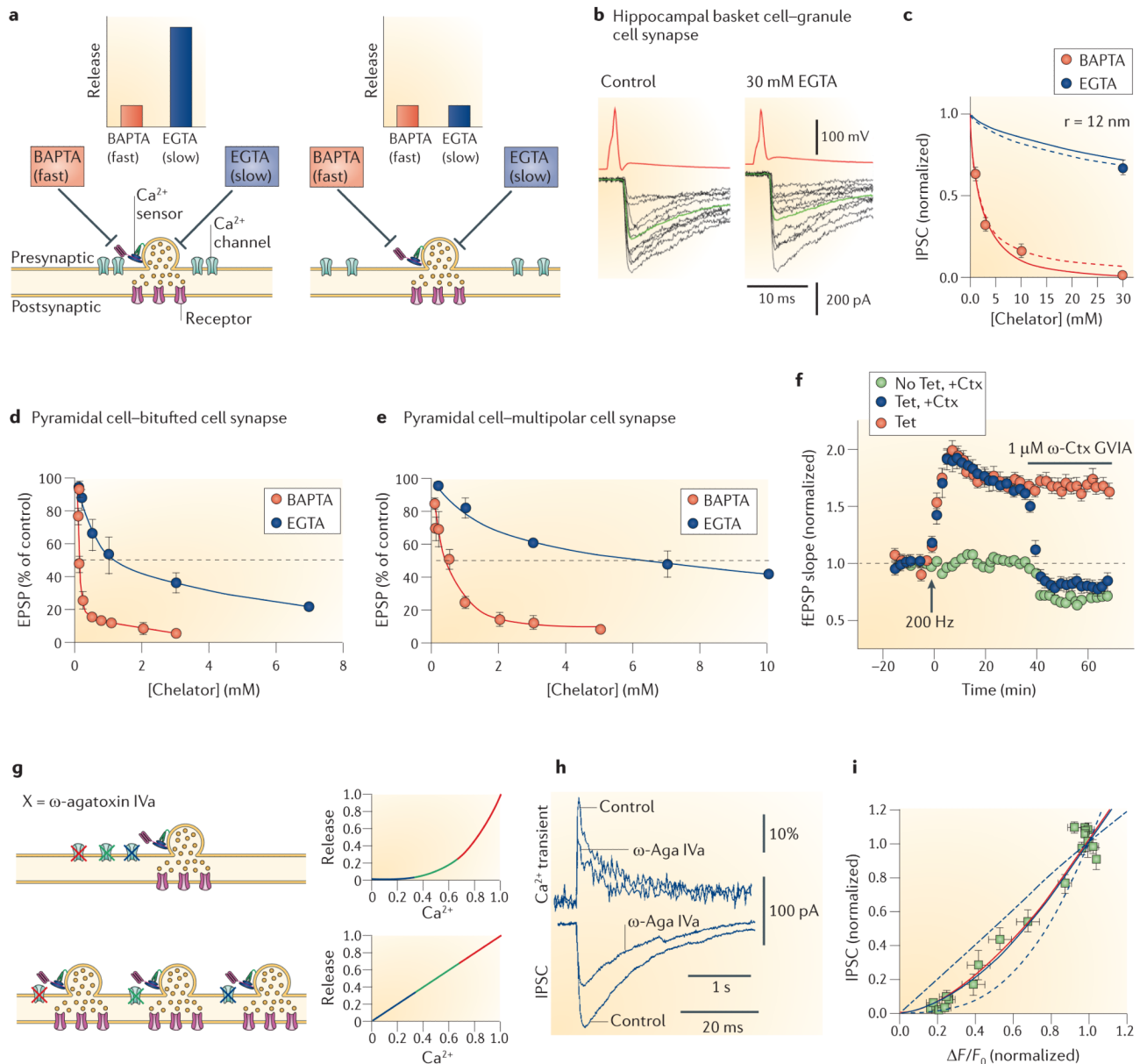


Figure 2. Experimental determination of the coupling distance and the number of open Ca^{2+} channels that mediate transmitter release

a | Ca^{2+} chelators with different on rates are used to probe the distance between Ca^{2+} channels and sensors. In a tight coupling regime (left), only the fast Ca^{2+} chelator BAPTA, but not the slow Ca^{2+} chelator EGTA, will capture the Ca^{2+} on its way from the source to the sensor. By contrast, in a loose coupling regime (right), both chelators will be effective, according to their affinity values, which are comparable. **b** | Effects of 30 mM EGTA on unitary inhibitory postsynaptic currents (IPSCs) at the hippocampal basket cell–granule cell synapse under steady-state conditions. Orange traces, presynaptic action potentials; black traces, IPSCs; green traces, averages. Note that EGTA has only minimal effects at this synapse. **c** | Concentration dependence of the effects of BAPTA and EGTA at the hippocampal basket cell–granule cell synapse. Lines represent predictions of a reaction–diffusion model simplified by linearization (continuous lines, predictions for a single Ca^{2+}

channel; dashed lines, predictions for a cluster of multiple Ca^{2+} channels). The best description of the experimental data was obtained assuming a coupling distance of 12 nm.

d,e | Target-cell-specific differences in the coupling distance. Concentration dependence of the effects of BAPTA and EGTA at glutamatergic synapses formed by pyramidal neurons in somatosensory cortex on bitufted interneurons (presumably representing somatostatin-positive subtypes) and multipolar interneurons (presumably representing parvalbumin-expressing subtypes). In the pyramidal neuron–multipolar interneuron synapses, synaptic transmission is only weakly sensitive to EGTA, suggesting tight coupling between Ca^{2+} channels and sensors.

f | Presynaptic plasticity changes the contribution of N-type Ca^{2+} channels to transmitter release at glutamatergic perforant path synapses on hippocampal CA1 pyramidal neurons. After 200 Hz tetanic stimulation (arrow, Tet), inducing a presumably presynaptic form of long-term potentiation, the amount of block by ω -conotoxin GV1a (ω -Ctx GV1a), a selective N-type channel blocker, increases, suggesting that transmission becomes increasingly dependent on N-type channels.

g | A slow calcium channel blocker can be used to estimate the number of open channels required for neurotransmission. In a multiple channel coupling scenario (upper panel), blocking Ca^{2+} channels with a slow blocker scales the Ca^{2+} transient at the vesicular Ca^{2+} sensor, reducing transmitter release supralinearly. In a single-channel scenario (lower panel), blocking Ca^{2+} channels sequentially eliminates channel–vesicle nanocomplexes, inhibiting transmitter release linearly.

h | Ca^{2+} transients (upper traces) and IPSCs (lower traces) at the hippocampal basket cell–granule cell synapse before and after application of ω -agatoxin IVa (ω -Aga IVa). Corresponding scale bars are at the bottom. Note that the toxin reduces Ca^{2+} transients and IPSCs to a comparable extent. Presynaptic Ca^{2+} transients were measured as relative fluorescence changes ($\Delta F/F_0$) using the Ca^{2+} indicator dye Oregon Green BAPTA1.

i | Plot of peak amplitudes of synaptic currents as a measure of exocytosis against $\Delta F/F_0$ as a measure of Ca^{2+} inflow (both normalized to the respective control value). The blue curves show the predictions of a binomial model of Ca^{2+} channel block with different numbers of open Ca^{2+} channels ($n = 1, 2$ or 10). The red curve shows free fit with a power function. Note that the best fit of the experimental observations can be obtained with a model assuming two or three Ca^{2+} channels.

Parts **b** and **c** are reproduced, with permission, from REF. 26 © (2008) Elsevier. Parts **d** and **e** are reproduced, with permission, from REF. 25 © (2001) Wiley-Blackwell. Part **f** is reproduced, with permission, from REF. 48 © (2009) Elsevier. Parts **h** and **i** are reproduced, with permission, from REF. 56 © (2010) Macmillan Publishers Ltd. All rights reserved. EPSP, excitatory postsynaptic potential; fEPSP, field EPSP.

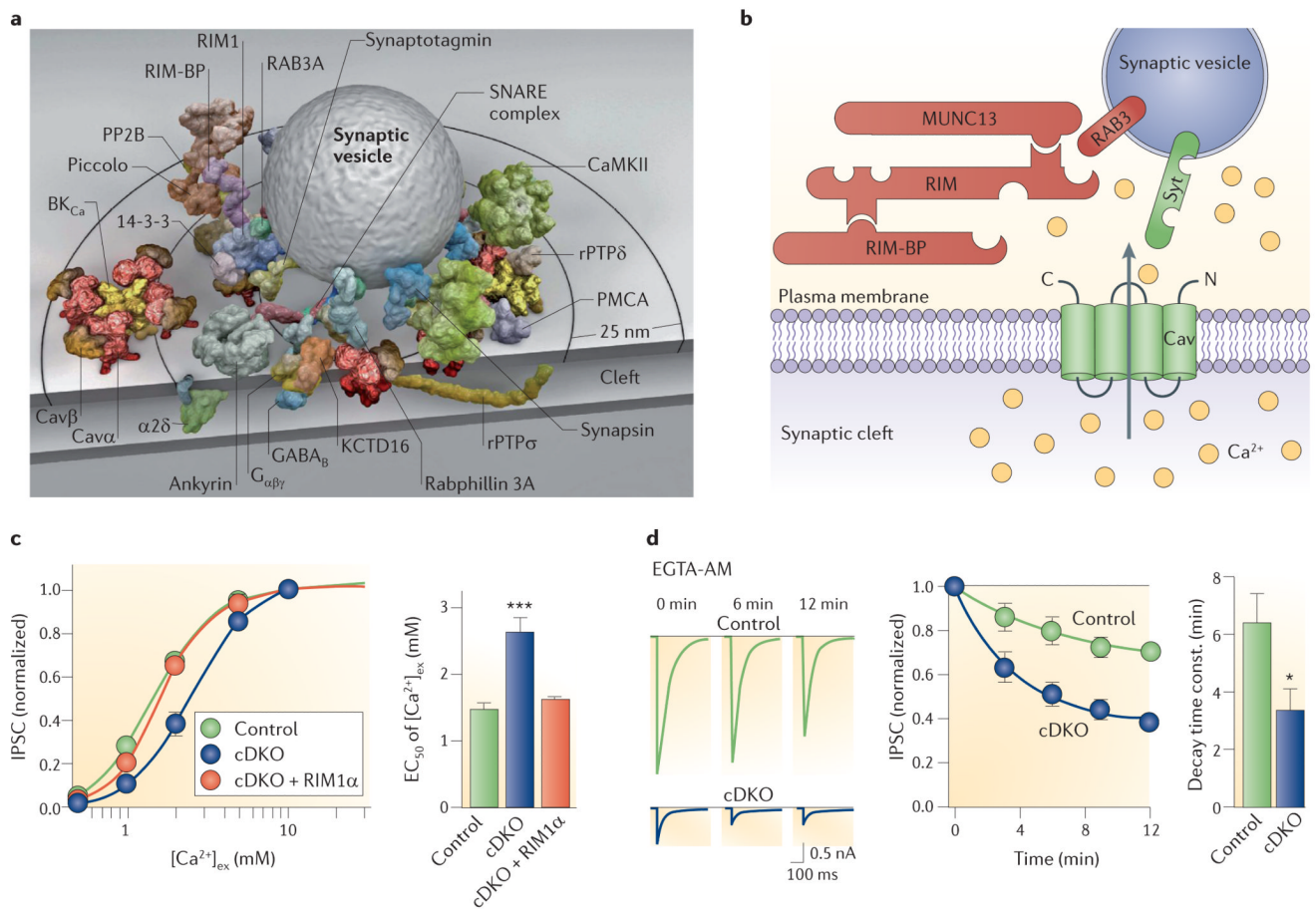


Figure 3. Molecular mechanisms of nanodomain coupling

a | Space filling models of protein complexes in the active zone. A synaptic vesicle is surrounded by several proteins. Only a single copy of each protein is depicted⁹⁴. **b** | Illustration of the proposed function of RAB3-interacting molecule (RIM) as a tether in the active zone. Both RIM and RIM binding protein (RIM-BP) bind to the C terminus (C) of the Ca²⁺ channel. Furthermore, the N terminus (N) of RIM binds to RAB3A. As RAB3A is a vesicular protein, the complex links Ca²⁺ channels to synaptic vesicles. **c** | Genetic elimination of RIMs changes the dependency of inhibitory postsynaptic current (IPSC) amplitudes on extracellular Ca²⁺ concentration at GABAergic synapses. Left, dose-effect curves in control synapses, RIM conditional double knockout (cDKO) synapses, and after rescue with recombinantly expressed RIM1 α (cDKO + RIM1 α). Right, summary bar graph of EC₅₀ (the concentration of an agonist at which 50% of the response is seen) values in the three conditions. **d** | Genetic elimination of RIMs changes the coupling between Ca²⁺ source and Ca²⁺ sensor at GABAergic synapses. Left, IPSCs in control synapses (top) and in RIM double knockout synapses (bottom) at different times during application of EGTA acetoxymethyl ester (EGTA-AM). Centre, time course of inhibitory effects of EGTA-AM at control synapses (green) and double knockout synapses (blue). Right, time constants of the onset of the effects of EGTA-AM. EGTA-AM acts more rapidly in the RIM double knockout mouse, suggesting a looser coupling between Ca²⁺ channels and sensors of exocytosis¹⁰⁵. Although the experiments were performed at cultured hippocampal inhibitory synapses, it is likely that at least a subset includes output synapses from parvalbumin-expressing, fast-spiking interneurons. Image in **a** is reproduced, with permission, from REF. 94 © (2010) PNAS. Part **b** is modified, with permission, from REF. 138 © (2011) Elsevier.

Parts **c** and **d** are reproduced, with permission, from REF. 105 © (2011) Elsevier. BK_{Ca}, large conductance calcium-activated potassium channel; CaMKII, calcium/calmodulin-dependent protein kinase type II; Cav, voltage-gated calcium channel; KCTD16, K⁺ channel tetramerization domain-containing protein 16; PMCA, plasma membrane Ca²⁺ ATPase; PP2B, protein phosphatase 2B; Syt, synaptotagmin; RAB3A, small G protein localized on synaptic vesicles; rPTP, receptor protein tyrosine phosphatase.

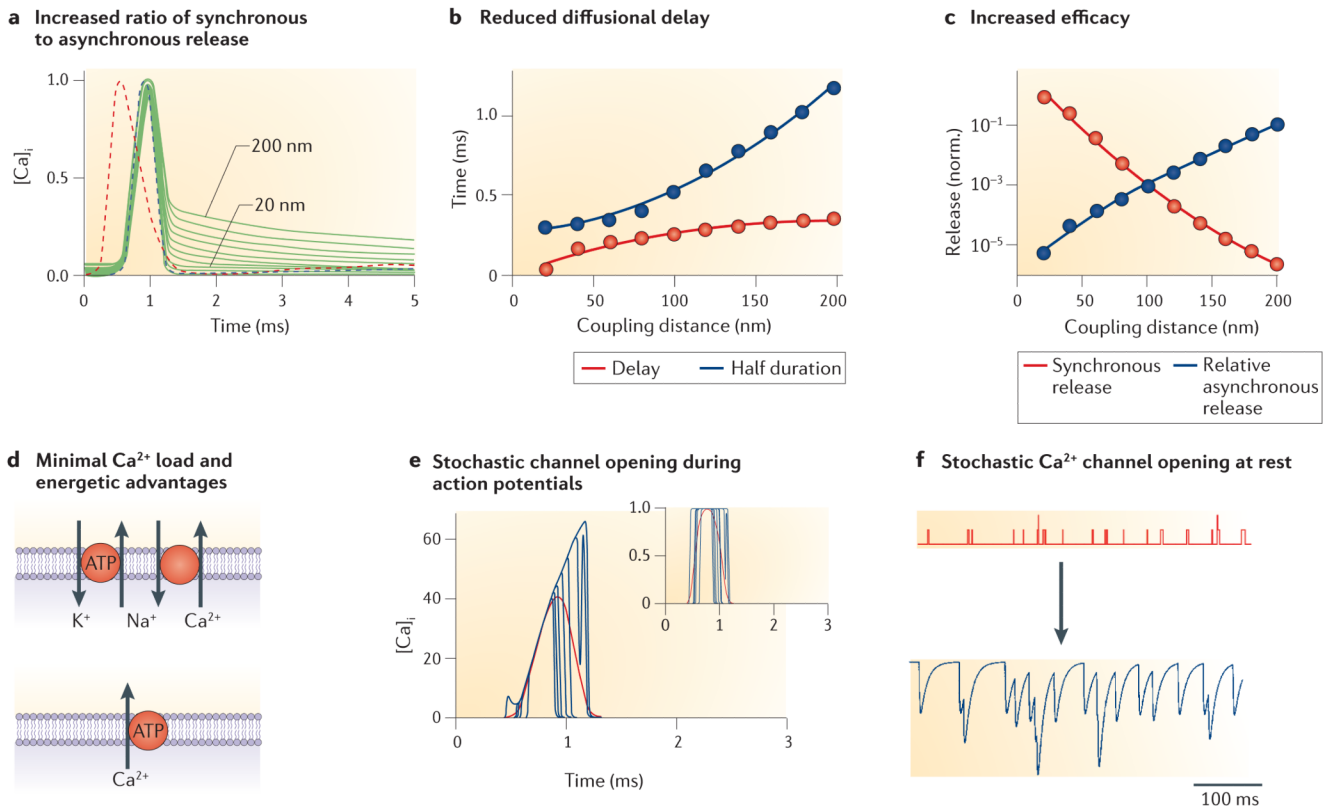


Figure 4. Functional consequences of nanodomain coupling

a | Tight coupling increases the ratio of synchronous to asynchronous release by increasing the ratio of peak Ca^{2+} to residual Ca^{2+} . Traces show normalized action potential-evoked Ca^{2+} transients at distances between 20 nm and 200 nm (step size 20 nm). The fast component of the Ca^{2+} transient will drive synchronous release, whereas the slow component will initiate asynchronous release. The red dashed line represents the presynaptic action potential. **b** | Tight coupling reduces the component of the synaptic delay that is caused by diffusion of Ca^{2+} (red circles and curve) and, in parallel, increases the temporal precision of release in relation to the presynaptic action potential ('half duration'; blue circles and curve). **c** | Tight coupling increases release probability and thus synaptic efficacy (red circles and curve) and, in relative terms, decreases asynchronous release (blue circles and curve). **d** | Tight coupling reduces the presynaptic Ca^{2+} load and thus introduces energetic advantages. Na^+/K^+ -ATPase, $\text{Na}^+/\text{Ca}^{2+}$ exchanger and Ca^{2+} -ATPase are depicted schematically. $\text{Na}^+/\text{Ca}^{2+}$ exchanger and Ca^{2+} -ATPase are the main Ca^{2+} extrusion mechanisms in the presynaptic plasma membrane¹²². The Ca^{2+} -ATPase is primary active, that is, directly dependent on the hydrolysis of ATP. The $\text{Na}^+/\text{Ca}^{2+}$ exchanger is secondary active. It exploits the Na^+ ion gradient previously generated by the Na^+/K^+ -ATPase, another primary active transport. Thus, both Ca^{2+} extrusion pathways require hydrolysis of ~1 ATP for the extrusion of 1 Ca^{2+} ion. **e** | Use of a small number of Ca^{2+} channels introduces stochastic components in Ca^{2+} channel opening and closing, without affecting the rising phase of corresponding Ca^{2+} transients. Main plot, simulated Ca^{2+} concentration 12 nm away from a single Ca^{2+} channel activated by an action potential. Inset, open probability of the single Ca^{2+} channel. Ten individual openings are shown superimposed. Red curves show a regime with an infinite number of Ca^{2+} channels for comparison. Note that the rising phases of the Ca^{2+} transients are similar, despite stochastic Ca^{2+} channel opening. Thus, the opening of the Ca^{2+} channels is stochastic, whereas the rising phase of the Ca^{2+} transients is

largely deterministic. **f** | Use of a small number of Ca^{2+} channels may lead to excessive miniature release due to stochastic Ca^{2+} channel opening. Upper schematics, spontaneous opening of presynaptic Ca^{2+} channels; lower schematics, hypothetical 'spontaneous' release events driven by channel openings. Parts **a–c** are reproduced, with permission, from REF. 26 © (2008) Elsevier. Part **e** is reproduced, with permission, from REF. 56 © (2006) Macmillan Publishers Ltd. All rights reserved. In **b** and **c**, transmitter release was simulated using a previously established release model⁸⁰⁻⁸².

Table 1
Physicochemical properties of exogenous and endogenous Ca²⁺ buffers

Chelator/Ca ²⁺ -binding protein	Ca ²⁺ -binding rate (k_{on})	Ca ²⁺ -unbinding rate (k_{off})	Affinity (K_D)	Refs
BAPTA [*]	$4 \times 10^8 \text{ M}^{-1} \text{ s}^{-1}$	88 s^{-1} [‡]	220 nM	22,33,139
EGTA [*]	$1 \times 10^7 \text{ M}^{-1} \text{ s}^{-1}$	0.7 s^{-1} [‡]	70 nM	22,77
Calbindin	$7.5 \times 10^7 \text{ M}^{-1} \text{ s}^{-1}$	29.5 s^{-1}	293 nM [‡]	77,79
Calretinin [§]	$1.8 \times 10^6 \text{ M}^{-1} \text{ s}^{-1}$ (T)	1.29 s^{-1} (T)	717 nM [‡]	78
	$3.1 \times 10^8 \text{ M}^{-1} \text{ s}^{-1}$ (R)	1.73 s^{-1} (R)	5.6 nM [‡]	
Calmodulin N-lobe [§]	$7.7 \times 10^8 \text{ M}^{-1} \text{ s}^{-1}$ (T)	$1.6 \times 10^5 \text{ s}^{-1}$ (T)	$208 \mu\text{M}$ [‡]	79
	$3.2 \times 10^{10} \text{ M}^{-1} \text{ s}^{-1}$ (R)	$2.2 \times 10^4 \text{ s}^{-1}$ (R)	688 nM [‡]	
Calmodulin C-lobe [§]	$8.4 \times 10^7 \text{ M}^{-1} \text{ s}^{-1}$ (T)	$2.6 \times 10^3 \text{ s}^{-1}$ (T)	$31 \mu\text{M}$ [‡]	79
	$2.5 \times 10^7 \text{ M}^{-1} \text{ s}^{-1}$ (R)	6.5 s^{-1} (R)	260 nM [‡]	

^{*} For the exogenous chelators, the Ca²⁺-binding rate (on rate) is ~40 times higher for BAPTA than for EGTA. By contrast, the affinity values are comparable; in fact the affinity is threefold lower for BAPTA than for EGTA.

[‡] This value was calculated using $K_D = k_{off}/k_{on}$.

[§] For the Ca²⁺-binding proteins calretinin and calmodulin, Ca²⁺ binding is highly cooperative. Therefore, rates are given separately for tense (T) and relaxed (R) conformations of the protein.

Table 2
Sensitivity to BAPTA and EGTA distinguishes between nanodomain and microdomain coupling

Synapse	Age* and species	BAPTA IC ₅₀ [‡] or PSC amplitude	EGTA IC ₅₀ [‡] or PSC amplitude	Refs
<i>Synapses with nanodomain coupling</i>				
Squid giant synapse	Adult squid	0.73 mM	>>80 mM	11
Mature calyx of Held	P16–18 mouse	1.3 mM	35.4 mM	23
Hippocampal basket cell–granule cell synapse	P18–21 rat	1.6 mM	61.5 mM	26
Hippocampal basket cell–granule cell synapse	P19–22 rat	63.9 ± 4.3% in 100 μM BAPTA-AM [§]	No effect in 100 μM EGTA-AM [§]	43
Cerebellar molecular layer interneuron–interneuron synapse	P14–20 rat	Unknown	97.5 ± 4.8% and 82.8 ± 11.3% in 20 μM EGTA-AM [§]	27
Cerebellar climbing fibre–Purkinje cell synapse	P8–20 rat	Unknown	103 ± 5% in 20 μM EGTA-AM [§]	120
Auditory hair cell ribbon synapse	P14–40 mouse	<<5 mM (almost complete block)	>>5 mM	37
Retinal bipolar cell ribbon synapse	P15–25 rat	2.2 mM	>>5–10 mM	140
<i>Synapses with microdomain coupling</i>				
Young calyx of Held	P8–12 mouse	1.3 mM	7.5 mM	23
Young calyx of Held	P8–10 rat	0.61 mM	13.3 mM	3,141
Layer 5–layer 5 neocortical synapse	P14–16 rat	0.7 mM	7.9 mM	24
Layer 2/3 pyramidal cell synapse on bitufted interneuron	P14–15 rat	0.1 mM	1 mM	25
Layer 2/3 pyramidal cell synapse on multipolar interneuron	P14–15 rat	0.5 mM	7 mM	25
CCK interneuron–granule cell synapse	P19–22 rat	Unknown	6.8 ± 3.8% in 100 μM EGTA-AM [§]	43
Cerebellar climbing fibre synapse, ectopic release on Bergmann glial cell	P8–20 rat	Unknown	67 ± 11% in 20 μM EGTA-AM [§]	120

EGTA-AM, EGTA acetoxymethyl ester; P, postnatal day; PSC, postsynaptic current.

* For the calyx of Held, P12 is an important reference point because it represents the onset of hearing.

[‡]IC₅₀ (concentration of an inhibitor at which 50% inhibition of the response is seen) values were either directly taken from references or calculated from the amount of block according to a Hill equation.

[§]AM forms of EGTA permeate cell membranes easily. Once the intracellular compartment is reached, the AM residue is cleaved by endogenous esterases, and the Ca²⁺ chelator is trapped intracellularly. Although the precise EGTA concentration is not known, it is thought that this trapping mechanism leads to a ~100-fold enrichment in comparison to the extracellular concentration²⁸.